

Tropospheric Ozone Production Pathways with Detailed Chemical Mechanisms

Dissertation zur Erlangung des akademischen Grades
des Doktors der Naturwissenschaften
am Fachbereich Geowissenschaften
an der Freien Universität Berlin

Vorgelegt von
Jane Coates
im Juli 2016



1. Gutachter: Prof. Dr. Mark Lawrence
2. Gutachter: Prof. Dr. Peter Builtjes

Abstract

Acknowledgements

Table of Contents

| | | |
|----------|--|-----------|
| 1 | Introduction | 1 |
| 1.1 | Ozone | 2 |
| 1.2 | Ozone Production Chemistry | 3 |
| 1.2.1 | Chemical Families | 5 |
| 1.2.2 | Reservoir Molecules | 5 |
| 1.2.3 | Volatile Organic Compounds | 6 |
| 1.2.4 | VOC Chemistry | 8 |
| 1.2.5 | VOC and NO _x Chemistry | 10 |
| 1.3 | Emissions of Ozone Precursors | 12 |
| 1.4 | Effects of Meteorology on Ozone Production | 12 |
| 1.5 | Research Questions | 13 |
| 2 | Methodology | 15 |
| 2.1 | Air Quality Modelling | 15 |
| 2.1.1 | Model Description and Setup | 17 |
| 2.2 | Chemical Mechanisms | 18 |
| 2.2.1 | Near-Explicit Chemical Mechanisms | 19 |
| 2.2.2 | Lumped Intermediate Chemical Mechanisms | 21 |

| | | |
|----------|---|-----------|
| 2.2.3 | Lumped Molecule Chemical Mechanisms | 23 |
| 2.2.4 | Lumped Structure Chemical Mechanisms | 27 |
| 2.3 | Using the Chemical Mechanisms in MECCA | 28 |
| 3 | Presentation of Papers | 31 |
| 3.1 | Paper 1: A comparison of chemical mechanisms using tagged ozone production potential (TOPP) analysis | 31 |
| 3.2 | Paper 2: | 33 |
| 3.3 | Paper 3: | 33 |
| 4 | Overall Discussion and Conclusions | 35 |
| 5 | Summary and Zusammenfassung | 37 |
| | References | 39 |
| 6 | Paper 1: A comparison of chemical mechanisms using tagged ozone production potential (TOPP) analysis | 49 |
| 7 | Paper 2: | 65 |
| 8 | Paper 3: | 67 |
| 9 | Publication List | 69 |
| | Appendix | 71 |

List of Tables

| | | |
|-----|---|----|
| 1.1 | Chemical Families commonly used in Tropospheric Chemistry (Seinfeld and Pandis, 2006) | 5 |
| 2.1 | General settings used for MECCA box model in this study | 18 |
| 2.2 | Chemical mechanisms used in the study. | 19 |
| 2.3 | Summary of the CRI v2 and its five reduced variants. | 23 |
| 2.4 | Explicitness of each of the lumped-molecule chemical mechanisms listed in Table 2.2 | 24 |
| 2.5 | Carbon bonds and mechanism species represented in CBM-IV and CB05. | 27 |

List of Figures

| | | |
|-----|--|----|
| 1.1 | what is this | 8 |
| 1.2 | Ozone isopleth plots for various initial concentrations of NO_x and a specified VOC mixture. Taken from (Jenkin and Clemitshaw, 2000). . | 10 |
| 1.3 | Air parcel evolution overlayed with ozone isopleth plots for various initial concentrations of NO_x and VOCs. Taken from (Sillman, 1999). . | 12 |
| 2.1 | Flowchart of VOC degradation represented by the MCM | 21 |

Chapter 1

Introduction

In many areas around the world, air pollution is the leading environmental health risk affecting both the human population and ecology. The effects of air pollution range from chronic to less severe health impacts to the general population, air pollution has been labelled carcinogenic by the International Agency for Research on Cancer (IARC, 2013), significant economic impacts due to reduced growth rates of vegetation run into billions of euros per year. Due to these impacts, many governed areas introduced limit values for the most common and severe air pollutants (EEA, 2015).

Air pollutants can be emitted directly into the atmosphere (*primary pollutants*) or formed from the chemical reactions of other pollutants (*secondary pollutants*). Over Europe, particulate matter (PM) and tropospheric ozone (O_3) are the most problematic with up to 93 and 98 % of Europe's urban population exposed to concentrations above the WHO guidelines (EEA, 2015).

Tackling the high levels of tropospheric ozone is a complex problem as it is secondary pollutant formed from the reactions of emitted nitrogen oxides ($NO_x \equiv NO + NO_2$) and volatile organic compounds (VOCs) in the presence of sunlight. The photochemical nature of ozone production also lends itself to large impacts from meteorological variables such as temperature and wind speed (Jacob and Winner, 2009). Despite reductions to ozone precursors, the EU target value for human health (the EU does not currently have a limit value for ozone) was exceeded in 65 % of the EU member states and Europe's target value for vegetation was exceeded in 27 % of the EU-28 agricultural areas (EEA, 2013).

Air quality (AQ) modelling is an important tool for predicting future air quality under different emission and meteorological scenarios. Adequately

representing the complexity of ozone production is an ongoing challenge for the modelling community. Representing the numerous inputs in a correct way that is computationally efficient to reproduce observed trends in tropospheric ozone is a challenge for AQ models.

In this work, we shall determine the effects of different representations of specific model inputs on simulated ozone production. The research questions addressed in this work, relate specifically to the representation of chemistry, inputs of VOC emissions and temperature on ozone production and are detailed further in Sect. 1.5. After determining the effects on ozone production, Chap. 4 frames these effects in the wider view of improving current state of the art AQ modelling of tropospheric ozone.

1.1 Ozone

Ozone is a constituent gas of the atmosphere found in the stratosphere and troposphere, however its atmospheric effects are very different in these distinct regions. About 90 % of the atmospheric ozone is present in the stratosphere with a peak mixing ratio of about 12 ppm (Seinfeld and Pandis, 2006). Stratospheric ozone absorbs the sun’s ultraviolet radiation with wavelengths between 280 and 315 nm, this is extremely important as excess UV radiation may cause skin cancer, cataracts and a suppressed immune system in humans and can also damage land and aquatic ecosystems (World Meteorological Organisation, 2011).

In contrast, tropospheric ozone, found close to the surface, is both a pollutant and a greenhouse gas. Increased levels of tropospheric ozone are harmful to humans, plants and other living systems, as high ozone exposure can lead to pulmonary problems in humans and can decrease both crop yields and forest growth (World Meteorological Organisation, 2011).

Globally, tropospheric ozone is formed mainly via photochemical production from the reactions of emitted VOCs and NO_x . However, the Stratosphere-Troposphere Exchange (STE), which transports ozone from the stratosphere into the troposphere, may also play a role. The STE is driven by the Brewer-Dobson circulation (Brewer, 1949; Dobson, 1956), a relatively slow circulation (weeks to months) due to planetary wave disturbances in the troposphere (Haynes et al., 1991). The circulation causes air to move downward from the stratosphere into the troposphere at the mid and high latitudes and is balanced by upward exchange at the tropics.

A spring-time peak in O_3 concentrations is common in the mid-latitudes of the Northern Hemisphere and the STE was thought to be responsible. However, it is only very rarely that O_3 originating via STE can influence tropospheric O_3 levels (Lelieveld and Dentener, 2000). It was later realised that this spring maximum is due to the photochemical reactions occurring in the Northern Hemisphere spring after the buildup of reservoir species over winter (Penkett and Brice, 1986). These reservoir species are oxidised photochemically at a faster rate due to the increase in temperature, moisture and sunlight.

Tropospheric O_3 is not only impacted by emission levels, it is also affected by meteorological variables such as temperature, number of hours of sunshine and wind as these impact transport, dry and wet deposition rates and also chemical reaction rates (Hess and Mahowald, 2009). Meteorology influences both regional and global O_3 (Hess and Mahowald, 2009), climate patterns such as El Niño are also known to impact O_3 levels in certain areas (Sudo and Takashi, 2001). The effects of meteorology on ozone production shall be presented in more detail in Sect. 1.4.

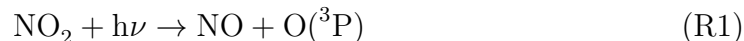
In general, there has been great effort to reduce emissions of ozone precursors from anthropogenic sources. For example, the emissions of non-methane VOCs (NMVOCs) over Europe have decreased by 20 % and emissions of NO_x have decreased by almost 30 % from 2004 levels. Despite these reductions in ozone precursors, up to 98 % of Europe’s urban population are exposed to levels of ozone exceeding the WHO guidelines (EEA, 2015).

Modelling of O_3 production has played a part in understanding the complexity of atmospheric chemistry, such as the non-linear relationship of O_3 production on the concentrations of VOCs and NO_x . The results of these modelling experiments can be used to produce more effective strategies for reducing ozone levels. The need for more effective air quality standards in turn also drives the model development and deeper understanding of the atmospheric processes controlling ozone production. In this work, we shall address the representation of three important parts of an AQ model (chemistry, NMVOC emissions and meteorology) and their impacts on simulated ozone production.

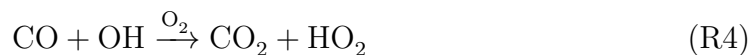
1.2 Ozone Production Chemistry

Tropospheric ozone is principally formed by the photolysis of nitrogen dioxide (NO_2), which produces nitrogen oxide (NO) and a ground state oxygen atom ($O(^3P)$),

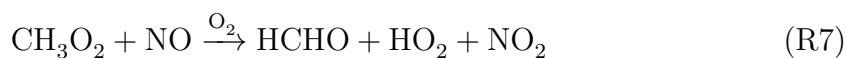
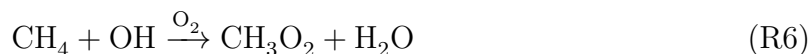
this then reacts with molecular oxygen (O_2) to form O_3 . Ozone reacts rapidly with NO to return NO_2 and O_2 , this is represented by the following reaction cycle.



These reactions do not produce net O_3 , due to a photoequilibrium between NO, NO_2 and O_3 (Atkinson, 2000). Adding VOCs of both biogenic and anthropogenic origin, such as methane (CH_4), and other gas-phase compounds, such as carbon monoxide (CO) - to the mix, results in net O_3 production. The oxidation mechanism of CO, taking into account reactions that give maximum O_3 yield, is



whilst the oxidation mechanism of CH_4 with maximum O_3 yield is



taking into account the net result for the CO oxidation mechanism, the net yield for CH_4 is Both mechanisms are taken from (Seinfeld and Pandis, 2006).

To summarise, oxidation of VOCs results in the formation of peroxy radicals which then convert NO to NO_2 and both (R1) and (R2) proceed. These oxidation mechanisms are linked in the sense that the CH_4 mechanism gives a maximum O_3 yield, once the mechanism of CO is also included.

Since these mechanisms produce the maximum O_3 yield, the reactions that cause O_3 destruction or inhibit its production are not included. It should also be noted that some reactions can follow more than one pathway that is indicated above and that products from these pathways can be removed from the atmosphere via deposition processes. Thus, the maximum O_3 yield outlined in reactions

Another aspect of O_3 production is its dependence on the atmospheric concentrations of both VOCs and nitrogen oxides ($NO_x = NO + NO_2$) and this also influences the reaction pathways. Moreover, the precursors of ozone are linked to

| Symbol | Family Name | Components |
|-----------------|---------------------|---|
| NO _x | Nitrogen oxides | NO + NO ₂ |
| O _x | Odd oxygen | O ₃ + O + O(¹ D) + NO ₂ + NO ₃ + N ₂ O ₅ |
| NO _y | Oxidised nitrogen | NO + NO ₂ + HNO ₃ + N ₂ O ₅ + ClONO ₂ + NO ₃ + HOONO ₂ + BrONO ₂ |
| HO _x | Hydrogen radicals | OH + HO ₂ |
| PAN | Peroxyacyl nitrates | Compounds of general formula RC(O)OONO ₂ |

Table 1.1: Chemical Families commonly used in Tropospheric Chemistry (Seinfeld and Pandis, 2006)

anthropogenic activity, hence a so-called weekend effect (i.e. there is a reduction on O₃ concentration over the weekend) is also evident (see for example, (Koo et al., 2012)). Further discussion on the balance of VOC and NO_x concentration to O₃ production shall be given in Section 1.2.5.

1.2.1 Chemical Families

A concept that is extremely useful in atmospheric chemistry is that of a chemical family. This is used to describe two or more compounds that form a rapid cycle of production and destruction. An example is the cycling between NO and NO₂ in (R1) and (R3), hence NO and NO₂ form the nitrogen oxides chemical family NO_x.

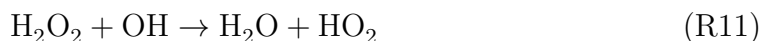
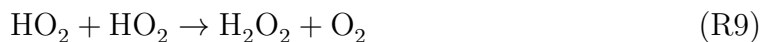
A chemical family also has its own chemical lifetime, where the chemical lifetime is the average time that a chemical species takes to be removed - by reaction or deposition processes - from the atmosphere. An equilibrium is reached for the compounds of the chemical family, called a pseudo-steady state, which is then re-balanced when a compound from the family reacts with a species not present in the chemical family.

Examples of important chemical families are given below in Table 1.1 and taken from (Seinfeld and Pandis, 2006).

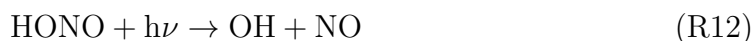
1.2.2 Reservoir Molecules

Compounds that react with radicals or NO_x are called reservoir molecules. These will slow down O₃ production and if they have a sufficiently long enough

lifetime, can also transport and then release radicals or NO_x to promote O_3 formation in a separate location. For example, hydrogen peroxide (H_2O_2) is a reservoir molecule for HO_x as shown in the below sequence of reactions (Seinfeld and Pandis, 2006).



Nitrous acid (HONO) is a reservoir molecule for NO_x and HO_x , formed by a heterogeneous reaction of NO_2 and H_2O . HONO can be formed during night-time and then photodissociates at sunrise to regenerate OH and NO (Seinfeld and Pandis, 2006).



An important class of reservoir molecules are the peroxyacyl nitrates (PANs) of general formula $\text{RC}(\text{O})\text{OONO}_2$. The first compound in this class, $\text{CH}_3\text{C}(\text{O})\text{OONO}_2$, is also called PAN and can be formed by reactions of peroxyacetyl radicals with NO_2 , PAN then thermally dissociates to return the reactants (Kleinman, 2005).



PAN's lifetime is dependent on meteorology due to a strong temperature dependence (Moxim et al., 1996). This can lead to situations where NO_x is transported to different regions and then released by dissociation. PAN is thought to have a regional rather than a global influence on the NO_x budget (Moxim et al., 1996).

1.2.3 Volatile Organic Compounds

Table lists Non-Methane Volatile Organic Compounds (NMVOCs) that are emitted from US cities (Baker et al., 2008). The mean is calculated from (Baker et al., 2008) using the total of 31 data points from 28 cities in the United States. Of these NMVOCs there is only one which has a primarily biogenic source and this is isoprene (2-methyl 1,3-butadiene). Although not evident from Table, biogenic VOCs are globally the most abundant VOCs (Goldstein and Galbally, 2007). Since the data in Table are mainly taken from urban cities, the impact of anthropogenic emissions

outweigh those of the biogenic sources (Baker et al., 2008) - although isoprene has some anthropogenic sources (see (Borbon et al., 2003)).

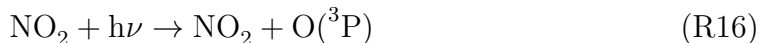
The sources of the alkanes listed below are natural gases, liquified petroleum gas (LPG), combustion and industry, for the case of octane, vehicle exhaust is also a source. Alkene sources are mainly due to industrial activities and vehicular emissions. Aromatic compounds are mainly due to vehicle emissions, while benzene and toluene are also emitted due to industrial activity and combustion is also a further source for benzene (Arsene et al., 2009).

Alkanes are saturated hydrocarbons, meaning that all bonds between carbon and hydrogen atoms are single bonds, resulting in slow reacting species. The dominant tropospheric process for alkanes is reaction with the hydroxyl (OH) radical, but they also react with the nitrate (NO_3) radical and chlorine atoms. The presence of a double bond in alkenes and a triple bond in alkynes leads to increased reactivity. In the troposphere both alkenes and alkynes react with the OH radical, the NO_3 radical and also with O_3 . Aromatic compounds react with the OH and NO_3 radicals. Hence it can be noted that the key reactive species in the troposphere is the OH radical as it reacts with practically all organic compounds, the exceptions being chlorofluorocarbons (CFCs) and halons without hydrogen atoms.

Reaction with the OH radical is predominant during the day, since it is formed mainly by photolysis, during the night there is an increase in the NO_3 radical concentration and so reaction rates with this radical are increased. The reason for this increased night-time concentration of the NO_3 radical is that during the day the reaction that forms NO_3



is balanced by the quick photolysis of NO_3



The main photolysis pathway is via reaction (R16) which occurs about 90 % of the time. However, during night-time photolysis does not occur and hence there is a buildup of NO_3 radicals (Atkinson, 1990, 2000).

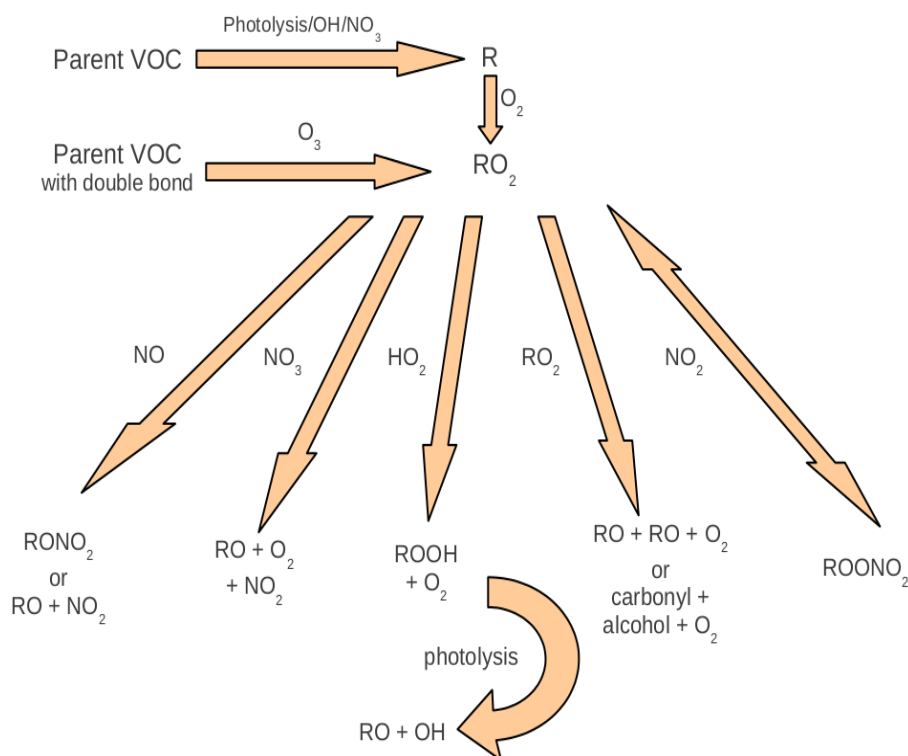
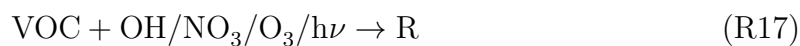


Figure 1.1: VOC reaction pathway

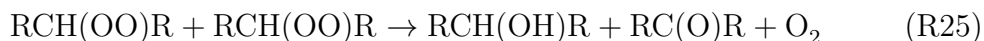
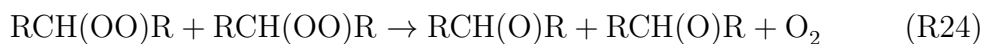
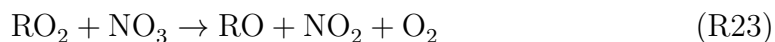
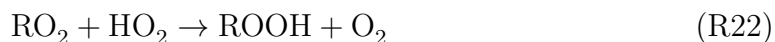
1.2.4 VOC Chemistry

Figure 1.1 represents a general and simplified reaction scheme for VOCs in the troposphere. Although there are many different VOC classes involved in tropospheric chemistry, there are many similarities between their reaction schemes. This shall be summarised below however for more a more detailed description of tropospheric chemistry, (Atkinson, 2000) should be consulted.

As noted earlier, the most common initiation reaction of a VOC is with the OH radical, and this forms an alkyl or substituted alkyl radical (R) depending on the parent VOC. The addition reaction with O₂ then leads to the formation of alkyl peroxy radicals (RO₂). During the night-time, reaction with the NO₃ radical is of importance and for VOCs containing a double bond, reaction with O₃ also occurs. Photolysis is an important degradation initiator for carbonyl species, this is particularly important throughout the whole degradation mechanism of the VOC as carbonyl species, such as formaldehyde, are common reaction products. These initial reaction pathways all lead to the formation of RO₂ radicals, as shown below.



RO₂ radicals can subsequently react with NO, NO₂, hydroperoxy (HO₂) radicals, NO₃ radicals - mainly during night-time - and also with other alkyl peroxy radicals. The competition between these reactions determines the amount of net ozone production or loss from the parent VOC.



All pathways in Figure 1.1 that lead to NO₂ formation can result in O₃ formation due to (R1) and (R2). Reaction with the HO₂ radical results in the formation of hydroperoxides (ROOH), which then photolyse to an alkoxy (RO) radical and the OH radical, this OH radical is then available to react with other VOCs. The carbonyl and alcohol products resulting from reaction with other RO₂ radicals will follow a similar sequence of reactions and hence can also produce further O₃. Reaction with NO₂ leads to the formation of alkyl peroxy nitrates (ROONO₂), however this reaction product can be thermally unstable and may decompose quickly to the reactants, as mentioned in Section 1.2.2.

The RO radical that results from many of the RO₂ pathways undergoes further reactions, either by decomposition, isomerisation or reaction with O₂. The products that result from the reaction pathways depend on the parent VOC and this also determines the number of NO-to-NO₂ conversions, eventually leading to O₃ formation.

All VOCs and their degradation products will ultimately result in carbon dioxide (CO₂) and water vapour. The path that each VOC takes to reach its final products is dependent on the type of VOC, the radical concentration, the NO_x concentration and other factors such as time of day and year. The detailed atmospheric chemistry of some simple VOCs is well-understood (for example, methane) however for more complex molecules, especially aromatic VOCs, there are a great number of uncertainties. These uncertainties can be related to kinetic data, photolysis rates, reaction branching ratios and in most cases the reaction products. Any uncertainties in reaction pathways and products of VOCs also leads to uncertainties in the ozone forming potential of the respective VOC (Atkinson,

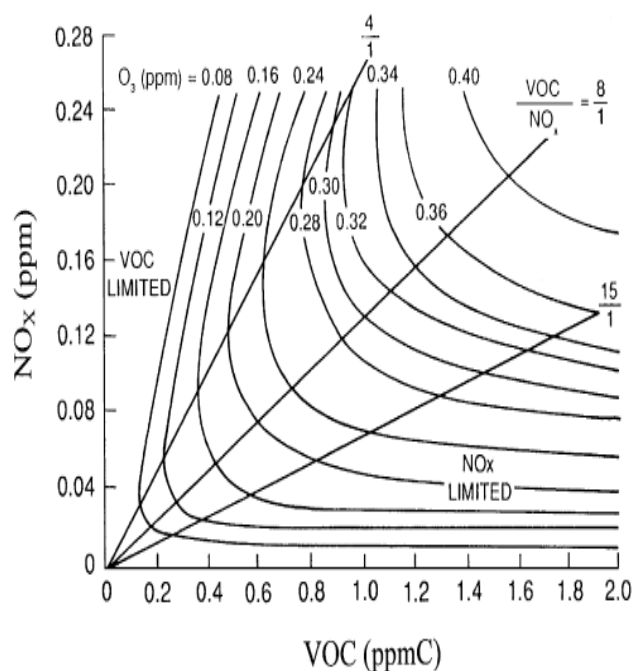


Figure 1.2: Ozone isopleth plots for various initial concentrations of NO_x and a specified VOC mixture. Taken from (Jenkin and Clemitshaw, 2000).

2000).

1.2.5 VOC and NO_x Chemistry

As mentioned above, O₃ chemistry is influenced by both VOC and NO_x concentrations. Figure 1.2 depicts the non-linear relationship between O₃ concentration when considered as a function of VOC concentration (in ppmC, i.e. parts per million mass of a carbon unit of the VOC, CH_{2.5}) and NO_x concentration (in ppm, i.e. parts per million mass).

This relationship can be divided into distinct regimes: **NO_x-sensitive**, **VOC-sensitive** and **VOC-and-NO_x-sensitive**. The NO_x-sensitive regime is the right-most part, the VOC-and-NO_x-sensitive regime is the middle section and the VOC-sensitive regime is the left-most part of Figure 1.2 and these correspond to high, middle and low VOC:NO_x ratios, respectively. These different regimes arise from how the atmosphere removes NO_x and radicals resulting from VOCs.

In the NO_x-sensitive regime, the concentration of NO_x is low compared to that of radicals. Hence, peroxy radicals are removed by reaction with the OH radical

such as



or by peroxy radical addition reactions.

This results in the NO concentration controlling the number of NO-to-NO₂ conversions, rather than the concentration of peroxy radicals produced during VOC oxidation. An increase in NO conversion would thus promote O₃ production due to an increase in (R1) and (R2) reactions. Increasing VOC concentrations would not increase O₃ production as this only speeds up the formation of peroxy radicals and has no direct effect on the NO_x concentration.

The VOC-sensitive regime corresponds to high NO_x concentrations, hence radicals will tend to react with either NO or NO₂. Increasing NO_x concentrations will not increase O₃ production as the NO_x will react with the peroxy radicals resulting from VOC degradation. However, this increase in NO_x increases the formation of nitric acid (HNO₃) by reaction with the OH radical (Kleinman, 1991, 1994; Kirchner et al., 2001).



The competition of VOCs and NO_x for reaction with the OH radical is at the heart of O₃ production or destruction in the VOC-sensitive regime. Reaction of VOCs with the OH radical will produce more peroxy radicals, increasing O₃ production whilst reaction of NO_x increases HNO₃ by (R27) which reduces O₃ production (Kleinman, 1991, 1994; Kirchner et al., 2001).

The VOC-and-NO_x-sensitive regime is characterised by O₃ production being sensitive to both VOC and NO_x concentrations. The turning point from a VOC-sensitive to a VOC-and-NO_x-sensitive regime is when the maximum O₃ production for a particular VOC concentration has been reached. The shift into a NO_x-sensitive occurs when increases in VOC concentrations result in very little O₃ production (Kirchner et al., 2001). The non-linear relationship can be thought of as a titration process between the amount of radicals and the NO_x present in the atmosphere.

This non-linear nature of the atmosphere must be taken into account when policymakers consider control strategies for O₃ concentrations. The difficulty is exacerbated by the fact that regions can alternate between these regimes depending on the season, time of day etc.

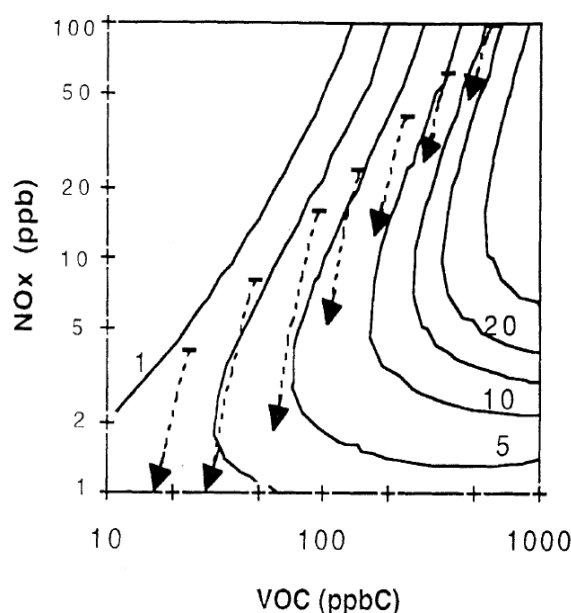


Figure 1.3: Air parcel evolution overlaid with ozone isopleth plots for various initial concentrations of NO_x and VOCs. Taken from (Sillman, 1999).

Moreover, an air parcel emitted in an urban area may also evolve as outlined in Figure 1.3, as it moves downwind. Once the air parcel has been emitted, it would typically fall into the VOC-sensitive regime but as the parcel ages it would move into the NO_x -sensitive regime. Reducing VOC and NO_x would reduce tropospheric O_3 , whilst reducing VOC levels would only be effective during VOC-sensitive regimes and reducing NO_x levels is only effective in NO_x -sensitive regimes and can even increase O_3 concentrations (Sillman, 1999). This is due to the radical or NO_x removal pathways that may or may not promote O_3 production as discussed above.

1.3 Emissions of Ozone Precursors

1.4 Effects of Meteorology on Ozone Production

The effect of meteorology is an aspect of atmospheric chemical transport modelling that needs to be taken into account. However it is also frequently the major source of uncertainty for the calculated O_3 concentrations. Wind speeds in particular may lead to under- or over-predicted values of O_3 concentrations (Sillman, 1999).

1.5 Research Questions

Chapter 2

Methodology

This chapter describes the methods and materials used throughout the study to address the research questions of the study (Section). Details of the modelling set-up, including initial and boundary conditions are included in this chapter.

add section
number

2.1 Air Quality Modelling

Photochemical models are used to predict future air quality scenarios. A large array of these models are used depending on the study focus, for example, global photochemical models can predict air quality on a global scale and include the relevant chemical and dynamical processes whereas an urban model focuses on a particular urban area and includes the relevant processes (such as topography, local emission source) to the area being studied. Despite differing scopes between models, there are a number of common inputs including emissions of chemical species into the model, transport of the species, atmospheric physical and chemical transformation and numerical solutions to the applicable differential equations.

Models are usually defined as either Eulerian or Lagrangian, with Eulerian models constituting most of the models used in the air quality modelling community (Russell and Dennis, 2000). Eulerian models describe the atmosphere by fixed computational cells where species enter in and out of the cell walls and the concentrations of the species within each cell are calculated as a function of time. Whilst Lagrangian models simulate changes of selected air parcels during advection through the atmosphere, hence there is no mass exchange between the surroundings and the air parcel (besides the emissions) and the model calculates concentrations at

different locations at different times (Seinfeld and Pandis, 2006).

Photochemical models also have different dimensions, ranging from zero-dimensional (box model) to three-dimensional models where the simplicity and computing power increase with the dimension of the model. 3-D models calculate atmospheric concentrations as a function of latitude, longitude, altitude and time. While 2-D models assume that concentration is a function of latitude and altitude (but not longitude) and time. Column models (or 1-D models) use concentrations that are a function of time and height. Box models are the simplest type of a model and have uniform atmospheric concentrations that are only a function of time (Seinfeld and Pandis, 2006).

Box models lack physical realism and essentially focus on processes relevant to a point in the atmosphere. Despite the lack of realism, box models are extremely useful for studying the detailed processes that influence air quality. Examples of modelling studies that have used box models include Qi et al. (2007), Li et al. (2014) and Nölscher et al. (2014).

All photochemical models numerically solve the chemical species conservation equation which describes the processes affecting the concentration of the different species:

$$\frac{\partial c_i}{\partial t} + \nabla \cdot \bar{U}c_i = \nabla \rho D \nabla (c_i/\rho) + R_i(c_1, c_2, \dots, c_n, T, t) + S_i(\bar{x}, t), \quad i = 1, 2, \dots, n. \quad (2.1)$$

In Eq. (2.1), c_i is the concentration (in mass or volume) of species i , \bar{U} is the wind velocity vector, D_i is the molecular diffusivity of species i , R_i is the rate of concentration change of species i through chemical reactions, $S_i(\bar{x}, t)$ is the source or sink of i at location \bar{x} , ρ is the air density and n is the number of predicted species. R may also be a function of meteorological parameters such as temperature T and S includes emission and deposition processes affecting i (Russell and Dennis, 2000).

re-word this
as too similar
to citation

The dimension and type of the model determine the set of differential equations that will be solved at each time step of the model run. Numerical methods to determine the concentration of species i in Eq. (2.1) vary between models, examples include Runge-Kutta (Sandu et al., 1997b), Finite Element (Russell and Dennis, 2000) or Rosenbrock methods (Sandu et al., 1997a).

Initial and boundary conditions are required to numerically solve the system of differential equations. Boundary conditions are typically the most difficult input to set accurately as this requires knowledge of the investigated species concentrations

and transport at the boundary edges (if applicable) of the model grid. Setting the initial conditions involves fixing the starting concentrations of the species being studied, these conditions are dependent on the area being studied and whether it is an urban or rural area, amongst other considerations.

2.1.1 Model Description and Setup

In order to assess the detailed processes producing tropospheric ozone within general air quality modelling, we used a box model to focus on the gas-phase chemistry affecting tropospheric ozone. All simulations in this study were performed using the MECCA (Module Efficiently Calculating the Chemistry of the Atmosphere) box model developed by Sander et al. (2005) that was adapted to include MCM v3.1 chemistry as described in Butler et al. (2011). The MECCA box model has been used for numerous detailed process studies of atmospheric gas-phase chemistry including Kubistin et al. (2010), Xie et al. (2008) and Lourens (2012).

MECCA is written using the FORTRAN programming language and runs on UNIX/Linux platforms. The setup of MECCA that we used uses the KPP (Kinetic Pre-Processor) (Damian et al., 2002) to efficiently setup up the system of differential equations (Eq. (2.1)). KPP processes the specified chemistry scheme in the chemical mechanism and generates Fortran code that is then compiled by MECCA. KPP also has numerous choices for the numerical solver used to numerically determine the concentrations of all the species described by the chemistry. We have used a Rosenbrock solver (the `ros3` option) throughout the study.

Aside from the chemistry, MECCA also calculates physical parameters at every time step of the simulations. In our simulations, the pressure, temperature, relative humidity and boundary layer height are held constant at the set values of Table 2.1. The specific changes to these parameters that were systematically varied to answer the research question related to are detailed in the relevant publication (Chapter).

add section

TBC about this

Photolysis rates in this study are calculated by using a paramaterisation that calculates the photolysis rate as a function of the solar zenith angle. This paramaterisation requires the degree of latitude for the study to be a defined variable in MECCA, we have chosen the 34° N latitude which is roughly that of the city of Los Angeles. The simulations start at the spring equinox (27th March) at 6am and allowed to run for seven diurnal cycles.

Table 2.1: General settings used for MECCA box model in this study

| Model Parameter | Setting |
|------------------------|------------------|
| Pressure | 1013 hPa |
| Temperature | 293 K |
| Relative Humidity | 81 % |
| Boundary Layer Height | 1000 m |
| Latitude | 34° N |
| Starting Date and Time | 27th March 06:00 |
| Model Time Step | 20 mins |
| Model Run Time | 7 days |

In our setup of MECCA, all fluxes into and out of the box are handled by KPP. The chemical mechanism file, processed by KPP, includes specific pseudo-unimolecular reactions specifying the emissions and dry deposition of chemical species along with the relevant rate. The chemical species that are emitted into the model and the emission rates are read into the model using a namelist file. Namelist files are also used to specify the initial conditions of chemical species and the mixing ratios of those chemical species that are fixed throughout the model. In all simulations, methane (CH_4) was fixed to 1.75 ppmv while carbon monoxide (CO) and O_3 are initialised at 200 ppbv and 40 ppbv and then allowed to evolve freely.

2.2 Chemical Mechanisms

The atmospheric chemistry in AQ models is described by the chemical mechanism used by the AQ model. The chemical mechanism includes rate coefficients, reaction pathways with the corresponding branching ratios, photolysis rates and reaction products which are required to solve the concentrations of each chemical species within the system using Equation (2.1).

Different modelling scopes and models determine the level of chemical detail of the chemical mechanism used by the AQ model, thus many different chemical mechanisms have been developed by the AQ modelling community. The level of detail included in the chemical mechanism determines the amount of computing resources required for the model simulations, hence the chemical mechanism in a 3-D model will typically be less detailed than the chemical mechanism used by a box model.

Chemical mechanisms range from highly-detailed (explicit) chemical mechanisms to the less-detailed lumped-structure and lumped-molecule chemical

Table 2.2: Chemical mechanisms used in the study.

| Chemical Mechanism | Lumping Type | Reference |
|--------------------|----------------------|--|
| MCM v3.1 and v3.2 | No lumping | Jenkin et al. (1997), Jenkin et al. (2003) Saunders et al. (2003), Bloss et al. (2005) Rickard et al. (2015) |
| CRIV2 | Lumped intermediates | Jenkin et al. (2008) |
| MOZART-4 | Lumped molecule | Emmons et al. (2010) |
| RADM2 | Lumped molecule | Stockwell et al. (1990) |
| RACM | Lumped molecule | Stockwell et al. (1997) |
| RACM2 | Lumped molecule | Goliff et al. (2013) |
| CBM-IV | Lumped structure | Gery et al. (1989) |
| CB05 | Lumped structure | Yarwood et al. (2005) |

mechanisms. The self-generating chemical mechanism of Aumont et al. (2005) is an example of an explicit chemical mechanism and includes many thousands of reactions outlining the degradation chemistry of VOCs, outlining even the reactions generating degradation products of minor importance in the atmosphere. Near-explicit chemical mechanisms, such as the Master Chemical Mechanism (MCM) of Jenkin et al. (1997), Jenkin et al. (2003), Saunders et al. (2003), are less-detailed than self-generating mechanisms but still contain many thousands of reactions and as such are mainly used in box models. The MCM representation of VOC degradation chemistry is discussed in more detail in Sect. 2.2.1.

Many other chemical mechanisms have been developed to describe atmospheric chemistry using less-detailed descriptions as those used by explicit and near-explicit chemical mechanisms so that these chemical mechanisms are computationally efficient for use within 3-D models. These reduced chemical mechanisms have been developed using a number of different techniques which ultimately lead to aggregating (lumping) VOC into mechanism species, these mechanism species are then degraded in such a way that the chemical production of ozone is similar to that from observational records. The first part of this study compares the maximal ozone produced from a number of reduced chemical mechanisms, listed in Table 2.2, a description of the different reduction techniques used by the reduced mechanisms is found in Sect. 2.2.2, Sect. 2.2.3 and Sect. 2.2.4. The main results from the chemical mechanism comparison study are presented in Sect. 3.1.

2.2.1 Near-Explicit Chemical Mechanisms

The Master Chemical Mechanism (MCM v3) is a near-explicit mechanism describing the chemical degradation of 107 non-aromatic VOCs in (Saunders et al.,

2003) and 18 aromatic VOCs in (Jenkin et al., 2003). The MCM v3.2 was used as the reference mechanism for this study as it was the most recent version of the MCM at the time of the first experiments related to the chemical mechanism study; the MCM v3.2 was obtained from the world wide web (<http://mcm.leeds.ac.uk/MCMv3.2/>). In total, the MCM v3.2 has 12,691 reactions including 4351 organic compounds and 46 inorganic compounds. The primary VOCs represented by the MCM v3.2 were determined by which VOC have the most emissions (by mass) as listed by the UK National Atmospheric Emissions Inventory and makes up about 70% of the mass emissions of unique species achieved.

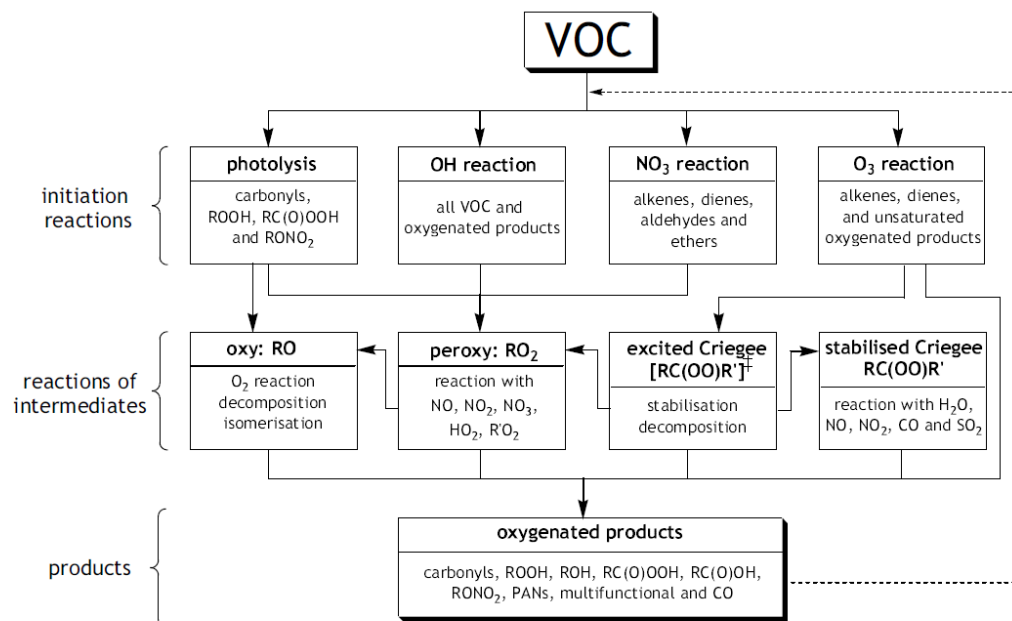
Each primary VOC and each degradation product, is individually degraded until it is broken down to CO_2 , H_2O , CO or an organic product (or radical) already represented by the MCM (Jenkin et al., 1997). Jenkin et al. (1997) outlines the main assumptions used when developing the MCM in order to reduce the number of chemical species and reactions, these include:

1. limiting the number of product channels resulting from reaction with the OH radical by disregarding pathways of low probability,
2. representing permutation (self and cross) reactions of organic peroxy radicals by a single parameterised reaction, and
3. simplifying the degradation chemistry, especially for those products deemed to be of minor importance.

Figure 2.1 shows the reaction pathways represented in the MCM of the primary VOC. The main reaction pathway for VOC degradation is by reaction with the OH radical, while ozonolysis is only important for alkenes, dienes, monoterpenes, some aromatic VOCs and some unsaturated oxygenated products. Reaction with the NO_3 radical is mainly important during the night-time and only included for alkenes, dienes, aromatics, aldehydes and ethers. Rate constants and branching ratios of the reactions represented in the MCM v3.2 are those recommended by IUPAC. If no data was available then they are estimated using structure activity representation (SAR) or group reactivity (GR) methods.

The degradation products of the primary VOCs are also treated in detail, with the first generation products also degraded further as part of the MCM. Those degradation products having significant tropospheric concentrations are treated in detail by the MCM otherwise the further degradation is limited to reaction with the OH radical. Those products deemed of minor importance are also greatly simplified whilst retaining product lifetimes and maintaining the carbon and nitrogen balance.

Figure 2.1: Flowchart of the major reactions of primary VOCs, intermediates and products considered in the MCM. Taken from Fig. 1 in Saunders et al. (2003)



2.2.2 Lumped Intermediate Chemical Mechanisms

Chemical mechanisms which aggregate (lump) the degradation products rather than primary VOC are called lumped intermediate chemical mechanisms. The Common Representative Intermediates (CRI) chemical mechanism (Jenkin et al., 2008) is an example of a lumped intermediate mechanism.

The CRI is a reduced version of the MCM that can be used in 3-D AQ models. Reducing the complexity of the MCM was achieved by representing many degradation products (intermediates) in the CRI by a single mechanism species, rather than lumping primary VOC into a mechanism species. These intermediates are designed to produce the same amount of ozone as when using the MCM. The CRI v2 was used in this study and the intermediates in this version of the CRI mirror the ozone production from the MCM v3.1.

The CRI v2 is available online (<http://mcm.leeds.ac.uk/CRI>) in a full version and further reduced variants that include even further reductions to the chemistry represented in MCM v3.1 by also lumping VOCs into lumped mechanism species. Jenkin et al. (2008) describes the main assumptions made in order to condense the organic chemistry of the MCM v3.1 to the lumped intermediate chemistry of the CRI v2, while Watson et al. (2008) describes the further reductions made to the

CRI v2 to produce the five lumped emission variants. The most reduced version of the CRI v2 has also been implemented into the widely used 3-D regional model WRF-CHEM as described in Archer-Nicholls et al. (2014).

The approach used to develop the CRI involves determining the potential number of NO-to-NO₂ conversions by the peroxy radicals formed during the degradation of a VOC, this is called the CRI-index. The CRI-index is thus the potential number of ozone molecules produced during the degradation of a VOC as the number of potential NO-to-NO₂ conversions by peroxy radicals is directly related to the potential number of O₃ molecules (Sect.). A single “common representative” is created to represent a part of the secondary degradation of a large number of species based on the CRI-index that was calculated based on the description of the degradation of the VOC in the MCM (Jenkin et al., 2008). This approach greatly reducing the number of species and reactions in the CRI compared to the near-explicit representation of the MCM.

The mechanism intermediate species are further optimised by performing multi-day model runs comparing the ozone produced from a single VOC in the CRI v2 to that in MCM v3.1. These model runs were performed for each of the primary VOC represented in the MCM v3.1 and CRI v2, starting with the smallest VOC of a particular functional group and only moving to the next largest VOC once the ozone production was optimised to that of the MCM v3.1. The primary criterion in these tests was ozone formation, the ozone formation of the mechanism intermediate species was optimised to that in the MCM v3.1 using a non-linear least squares fitting and the agreement was improved by varying the OH-reactivity and photolysis rate of the intermediate species. The individual testing of the intermediates for each VOC also showed that some intermediates did not directly follow the CRI-index rule and in-place adjustments were required to retain the ozone formation in the MCM v3.1. This approach was used for OH, O₃ and NO₃ initiated degradation (Jenkin et al., 2008).

Despite the large reductions to the MCM v3.1 chemistry to produce the CRI v2 described in Jenkin et al. (2008), the number of reactions are still too many to guarantee computational efficiency for use in 3-D models. Further reductions were made by lumping VOC emissions to produce five further reduced variants of the CRI v2; the methodology for these reductions is described in Watson et al. (2008) and summarised below.

The focus of the reductions to the full CRI v2 was on reducing the number of species and reactions representing anthropogenically emitted VOC, as on a global

Table 2.3: Summary of the CRI v2 and its five reduced variants. Data from Table 1 in Watson et al. (2008).

| CRI version | v2 | v2-R1 | v2-R2 | v2-R3 | v2-R4 | v2-R5 |
|------------------------|-------------|-------------|-----------|-----------|-----------|-----------|
| Primary VOCs | 115 | 67 | 55 | 42 | 33 | 22 |
| Species ^a | 434(4361) | 373(3466) | 352(3099) | 296(2649) | 219(1983) | 195(1244) |
| Reactions ^a | 1183(12775) | 1012(10150) | 988(9099) | 882(7833) | 643(5884) | 555(3670) |

^a Data in brackets represents the number of species and reactions required to degrade the same VOCs in the MCM v3.1.

scale these VOC are less significant than biogenically emitted VOC. The primary VOC represented by the full CRI v2 were reduced into lumped species based upon two methods, first by re-distributing VOCs of minor importance into lumped mechanism species that represent the chemistry of separate functional classes (alkane, alkene, aromatic, alcohol/ether, aldehyde, ketone, ester/acid). POCPs of the primary VOC being lumped into mechanism species were used to determine the ozone production from the primary VOC and then select the appropriate mechanism species. This approach created three reduced variants (CRI v2-R1, CRI v2-R2 and CRI v2-R3), with progressively increased lumping of the primary VOC (Watson et al., 2008).

The second approach to reducing the CRI v2 chemistry involved stricter reductions by using definitions of individual VOC emissions from the Global Emissions Inventory Activity (GEIA). Again, POCP values of the individual VOC were used to assign the lumped mechanism species. This approach produced the two most reduced variants of the CRI v2—CRI v2-R4 and CRI v2-R5, where the latter is the most reduced form of the CRI v2 (Watson et al., 2008). A summary of the five reduced variants of the CRI v2 compared to the full CRI v2 is presented in Table 2.3.

2.2.3 Lumped Molecule Chemical Mechanisms

Lumped molecule chemical mechanisms reduce atmospheric chemistry by aggregating primary VOC into mechanism species; this is the most common technique used when developing a reduced chemical mechanism. Different chemical mechanisms use different approaches when creating these mechanism species that are used represent a multitude of primary VOC. Typically NMVOC, such as isoprene, ethane and ethene, that make up a large fraction of NMVOC emissions are represented by dedicated (explicit) species and mechanism species are used to represent specific groups of NMVOC. These lumped mechanism species typically represent NMVOC based on functional group or OH-reactivity. Table 2.2 lists the lumped-molecule chemical mechanisms used in this study and Table 2.4 provides further information about these chemical mechanisms.

Table 2.4: Explicitness of each of the lumped-molecule chemical mechanisms listed in Table 2.2

| Chemical Mechanism | Number of Primary VOC | Number of Species | Number of Reactions |
|---------------------------|------------------------------|--------------------------|----------------------------|
| MOZART-4 | 20 | 85 | 157 |
| RADM2 | 21 | 63 | 157 |
| RACM | 25 | 77 | 237 |
| RACM2 | 40 | 120 | 363 |

MOZART

The Model for OZone and Related chemical Tracers (MOZART) chemical mechanism is an example of a lumped molecule chemical mechanism used in global and regional 3-D models. MOZART was developed for global chemical transport models and describes chemical processes within the boundary layer, free troposphere and stratosphere. MOZART-4 (Emmons et al., 2010) is the version used in this study and includes updates to the tropospheric chemistry from the previous MOZART-2 version (Horowitz et al., 2003); MOZART-3 (Kinnison et al., 2007) provided updated stratospheric chemistry.

MOZART-4 represents organic VOCs of methane, ethane, propane, ethene, propene, isoprene and formaldehyde by explicit species. Lumped mechanism species, BIGALK, BIGENE and TOLUENE, are used to represent alkanes and alkenes with four or more carbon atoms and all aromatic VOC (Emmons et al., 2010). Thus, the lumping species used by MOZART are based on the functionality of the VOC. There are no mechanism species representing emissions of esters, ethers or chlorinated NMVOC, when representing emissions of these less-reactive NMVOC are added to the BIGALK mechanism species as this has the slowest OH-reactivity.

MOZART-4 is also capable of representing aerosol chemistry and directly calculating both photolysis and dry deposition rates. For the purpose of this study, we were only interested in gas-phase chemical processes occurring with the boundary layer and so all processes relating to stratospheric, free troposphere and aerosol processes were not used. We also used the MCM approach to calculating photolysis and dry deposition rates.

RADM2

One of the older lumped molecule, but still widely used, chemical mechanisms is the second version of the Regional Acid Deposition Model (RADM2)

originally described in Stockwell et al. (1990). RADM2 is typically used in regional modelling studies and the chemical mechanism has been used extensively since its inception.

The organic VOC methane, ethane, ethene, isoprene and formaldehyde are represented explicitly in RAMD2. RADM2 uses lumped mechanism species to represent many VOC based upon the OH-reactivity and functional group of the VOC. In particular, there are three mechanism species (HC3, HC5, HC8) representing three types of hydrocarbons based on their OH-reactivity. These three species are then used to not only represent alkanes, but also many other species – such as alcohols, ethers, chlorinated VOC – based on their OH-reactivity.

All alkenes having more than two carbons are represented by either OLT or OLI depending on the position of the double bond (OLT: terminal alkenes and OLI: internal alkenes). The exception to this is isoprene, whose degradation is treated by an explicit species, due to the importance of isoprene chemistry as it is globally the VOC with the most emissions.

Aromatic VOC are represented by TOL, XYL or CSL depending on whether their OH-reactivity is slow, fast or they are hydroxy-substituted. Carbonyls (aldehydes and ketones) and organic acids are also represented by lumped mechanism species. Typically the NMVOC having the least number of carbons (e.g. formaldehyde and formic acid) is represented by an explicit species and then all other species from that functional group are represented by a lumped species.

The reaction rate coefficients of the lumped mechanism species were obtained by using a weighted mean of all the rate coefficients of the organic species aggregated into the model species, this was done to account for the difference in reactivities between the model and chemical species. The secondary degradation of the lumped species is described by chemistry that takes into account all the known VOC that are represented by the lumped species.

RADM2 reduces the number of peroxy radicals that need to be represented by using an operator species (XO2) that converts NO to NO₂ in an attempt to replicate the ozone produced by NMVOC when represented by the mechanism species. Thus, XO2 is one such mechanism species that appears in the secondary degradation of most of the lumped mechanism species. Another way of reducing the number of peroxy radicals is that only reactions of RO₂ with HO₂, CH₃O₂ and CH₃CO₃ are included as these are the most abundant RO₂.

RACM

Stockwell et al. (1997) describes the Regional Atmospheric Chemistry Mechanism (RACM) which is an updated to the RADM2 chemical mechanism. RACM includes lumped mechanism species not included in RADM2 such as API and LIM to represent cyclic terpenes with one double bond and all other cyclic terpenes.

Once again, the primary VOC are grouped into lumped mechanism species based upon functional group similarity and OH radical reactivity. The final mechanism species was determined by first grouping hundreds of anthropogenic VOCs into 32 emission categories and then finally aggregating into the final 16 lumped mechanism species.

The secondary chemistry of many of the lumped mechanism species included in both RADM2 and RACM was extensively updated which meant the inclusion of many new and additional mechanism species produced during the degradation of these lumped primary species. These product species are calculated as a weighted mean of the product yields of all the chemical species represented by the model species, where the individual yields are taken from literature.

The same approach to representing RO_2 - RO_2 reactions as used in RADM2 is used in RACM. Further details for calculating the reaction rate coefficients are described in Kirchner and Stockwell (1996).

RACM2

RACM was further extended and updated to RACM2, described in Goliff et al. (2013), once again the main updates included more lumped mechanism species to represent primary VOC emissions as well as updates to the secondary chemistry of lumped mechanism species. Alkane and alkene chemistry is largely unchanged from RACM except for some updates to reaction rate coefficients. Moreover, there were no major changes to the approach used when describing gas-phase chemistry from RADM2 or RACM.

Aromatic VOC and subsequent secondary chemistry was overhauled in RACM2 from RACM. RACM2 represents aromatic VOC by eight mechanism species instead of three species as in RACM, with explicit representation of benzene and each xylene isomer having its own mechanism species. The secondary chemistry of the aromatic VOC was updated to be similar to that of the MCM, with differences arising from the different treatments of gas-phase chemistry in the MCM and RACM2. The

Table 2.5: Carbon bonds and mechanism species represented in CBM-IV and CB05.

| Mechanism Species | Carbon Bond |
|-------------------|-------------|
| PAR | C–C |
| OLE | C=C |
| ALD2 | C=O |

main difference is the different treatment of $\text{RO}_2\text{-RO}_2$ reactions.

Acetone and methyl ethyl ketone (MEK) are now treated as separate species rather than being represent as a single mechanism species, KET, in RADM2 and RACM. Alcohols are now also represented in RACM2, whereas in the previous versions, alcohols were represented by HC3, HC5 or HC8.

2.2.4 Lumped Structure Chemical Mechanisms

The technique used by lumped-structure chemical mechanisms to reducing atmospheric chemistry is to express VOC emissions as permutations of building blocks that represent the structure of the emitted VOC. Thus, each lumped-structure chemical mechanism includes a number of these building blocks which are then emitted according to the initial VOC emissions being studied. The Carbon Bond mechanism is the most widely used lumped-structure chemical mechanism and in the first part of this thesis we have looked at the fourth version (CBM-IV, (Gery et al., 1989)) and the fifth version (CB05, (Yarwood et al., 2005)). Both Carbon Bond versions include mechanism species representing the different carbon bonds present in typically emitted VOC, the representation of the carbon bonds included in CBM-IV and CB05 are outlined in Table 2.5.

CBM-IV

The fourth version of the Carbon Bond mechanism was developed to represent the chemistry producing ozone in polluted urban conditions and is described in Gery et al. (1989). CBM-IV represents 20 organic species and requires 46 reactions to fully represent the secondary chemistry. Explicitly represented emitted NMVOC are those with the most significant emissions: isoprene, ethene and formaldehyde. In addition to the mechanism species listed in Table 2.5, there are mechanism species representing both slower and faster reacting aromatic VOC (TOL and XYL). Acetaldehyde (ALD2) is also represented as it is an important degradation product of the secondary chemistry from a number of VOC. CBM-IV uses an operator species

(XO2) to represent NO to NO₂ conversion by organic peroxy radical, similar to many lumped-molecule chemical mechanisms.

NMVOC emissions emitted by the mechanism species are described in Hogo and Gery (1989). For example, if heptane, having seven carbons each with a single bond, has emissions of 1×10^9 molecules cm⁻³ s⁻¹ then using the CBM-IV, these emissions would be represented by 7 PAR and thus PAR emissions would be 7×10^9 molecules cm⁻³ s⁻¹. Also, propene is represented as 1 OLE and 1 PAR and so emissions of 1×10^9 molecules cm⁻³ s⁻¹ would be emitted as 1×10^9 molecules cm⁻³ s⁻¹ of OLE and 1×10^9 molecules cm⁻³ s⁻¹ of PAR.

CB05

CBM-IV was updated to CB05, described in Yarwood et al. (2005), to include more species representing emitted VOC. CB05 now includes 99 organic reactions to represent the degradation of 37 organic species. Mechanism species for terpenes (TERP), ethane (ETHA), aldehydes with more than three carbons (ALDX), methanol (MEOH), ethanol (ETOH) and alkenes with both internal (IOLE) and external (OLE) double bonds were included.

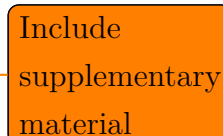
In addition to updating reaction rate constants and including more mechanism species to represent atmospheric chemistry more explicitly, the CB05 was also updated to include chemistry reflecting low-NO_x conditions. Thus reactions involving peroxide formation, a characteristic of low-NO_x conditions, were included in CB05.

2.3 Using the Chemical Mechanisms in MECCA

As outlined in Sect. 2.1.1, the MECCA boxmodel is based upon the KPP pre-processor and so required that all chemical mechanisms listed in Table 2.2 be written in the KPP format. The KPP format of each chemical mechanism was either obtained from the WRF/Chem (Grell et al., 2005) model, which includes KPP files of RADM2, RACM and CBM-IV for use within the model. For all the other chemical mechanisms, the chemistry published in the original reference were adapted to the KPP format.

Some changes were made to the original chemistry specified by each chemical mechanism. Firstly, the inorganic chemistry of the MCM v3.2 was used in each

chemical mechanism in order to focus on differences between chemical mechanisms of their representation of the secondary degradation chemistry of emitted NMVOC. Other changes included adopting the MCM v3.2 approaches to photolysis and peroxy-peroxy reactions, a more detailed description of these changes are found in the supplementary material of the first paper of this thesis (Chap. 6).



Include
supplementary
material

Chapter 3

Presentation of Papers

This chapter will outline the main findings in each of the scientific papers that were published as part of the PhD.

3.1 Paper 1: A comparison of chemical mechanisms using tagged ozone production potential (TOPP) analysis

Published: J. Coates and T. M. Butler. A comparison of chemical mechanisms using tagged ozone production potential (TOPP) analysis. *Atmospheric Chemistry and Physics*, 15(15):8795–8808, 2015. doi:10.5194/acp-15-8795-2015. URL <http://www.atmos-chem-phys.net/15/8795/2015/>.

The first paper described a box modelling study in which the secondary chemistry represented in many reduced chemical mechanisms (Table) for VOC

 typical of urban environments (Table 2 of the article) were compared to the detailed MCM chemical mechanisms. The research question addressed in this paper was to verify whether these different representations of this secondary chemistry influence ozone production.

The degradation of each VOC prescribed in each chemical mechanism was “tagged” so that the O_x production, a proxy for O_3 production, could be attributed to the individual VOC sources. Tagging the chemical mechanisms involved labelling every organic degradation product from a VOC with the name of the emitted VOC,

thus each VOC has a separate set of reactions fully describing its degradation until the final products, CO_2 and H_2O , are produced.

The ozone mixing ratios from reduced chemical mechanisms were generally lower than the mixing ratios from the reference MCM chemical mechanisms on the first two days of the simulations. The VOC degradation prescribed in CRI v2, a lumped-intermediate mechanism, produced the most similar amounts of O_x to the MCM v3.2 for each VOC. Thus, the approach of using lumped-intermediate species whose degradation are based upon more detailed chemical mechanisms is preferable when developing future chemical mechanisms.

Many VOC are broken down into smaller-sized degradation products faster on the first day in reduced chemical mechanisms than the MCM v3.2 leading to lower amounts of larger-sized degradation products that can further degrade and produce O_x . Thus, many VOC in reduced chemical mechanisms produce a lower maximum of O_x than the MCM v3.2 ultimately leading to lower O_3 mixing ratios from the reduced chemical mechanisms compared to the MCM v3.2.

Reactive VOC, such as unsaturated aliphatic and aromatic VOC, produce maximum O_x on the first day of the simulations. Unsaturated aliphatic VOC produce similar amounts of O_x on the first day between mechanisms; differences in O_x production arise when mechanism species are used to represent individual VOC. Large inter-mechanism differences in O_x production result from the degradation of aromatic VOC on the first day due to the faster break down of the mechanism species representing aromatic VOC in reduced chemical mechanisms.

The less-reactive alkanes produce maximum O_x on the second day of simulations and this maximum is lower in each reduced chemical mechanism than the MCM v3.2 due to the faster break down of alkanes into smaller sized degradation products on the first day. The lower maximum in O_x production during alkane degradation in reduced mechanisms would lead to an underestimation of the O_3 levels downwind of VOC emissions, and an underestimation of the VOC contribution to tropospheric background O_3 when using reduced mechanisms in regional or global modelling studies.

3.2 Paper 2:

3.3 Paper 3:

Chapter 4

Overall Discussion and Conclusions

Chapter 5

Summary and Zusammenfassung

References

- C. Appenzeller, J. R. Holton, and K. H. Rosenlof. Seasonal variation of mass transport across the tropopause. *Journal of Geophysical Research*, 101(D10):15,071–15,078, 1996.
- S. Archer-Nicholls, D. Lowe, S. Utembe, J. Allan, R. A. Zaveri, J. D. Fast, Ø. Hodnebrog, H. Denier van der Gon, and G. McFiggans. Gaseous chemistry and aerosol mechanism developments for version 3.5.1 of the online regional model, WRF-Chem. *Geoscientific Model Development*, 7(6):2557–2579, 2014. doi:10.5194/gmd-7-2557-2014. URL <http://www.geosci-model-dev.net/7/2557/2014/>.
- C. Arsene, A. Bougiatioti, and N. Mihalopoulos. Sources and variability of non-methane hydrocarbons in the Eastern Mediterranean. *Global NEST Journal*, 11(3):333–340, 2009.
- R. Atkinson. Gas phase tropospheric chemistry of organic compounds: a review. *Atmospheric Environment*, 24A(1):1–41, 1990.
- R. Atkinson. Atmospheric chemistry of VOCs and NO_x. *Atmospheric Environment*, 34(12-14):2063–2101, 2000.
- B. Aumont, S. Szopa, and S. Madronich. Modelling the evolution of organic carbon during its gas-phase tropospheric oxidation: development of an explicit model based on a self generating approach. *Atmospheric Chemistry and Physics*, 5(9):2497–2517, 2005. doi:10.5194/acp-5-2497-2005. URL <http://www.atmos-chem-phys.net/5/2497/2005/>.
- A. K. Baker, A. J. Beyersdorf, L. A. Doezema, A. Katzenstein, S. Meinardi, I. J. Simpson, D. R. Blake, and F. S. Rowland. Measurements of nonmethane hydrocarbons in 28 United States cities. *Atmospheric Environment*, 42:170–182, 2008.
- C. Bloss, V. Wagner, M. E. Jenkin, R. Vollamer, W. J. Bloss, J. D. Lee, D. E. Heard, K. Wirtz, M. Martin-Reviejo, G. Rea, J. C. Wenger, and M. J. Pilling. Development

of a detailed chemical mechanism (MCMv3.1) for the atmospheric oxidation of aromatic hydrocarbons. *Atmospheric Chemistry and Physics*, 5:641–664, 2005.

A. Borbon, H. Fontaine, N. Locoge, M. Veillerot, and J. C. Galloo. Developing receptor-oriented methods for non-methane hydrocarbon characterisation in urban air - Part I: source identification. *Atmospheric Environment*, 37:4051–4064, 2003.

A. W. Brewer. Evidence of a world circulation provided by the measurements of helium and water vapour distribution in the stratosphere. *Quarterly Journal of the Royal Meteorological Society*, 75(326):351–363, 1949.

T. Butler, M. Lawrence, D. Taraborrelli, and J. Lelieveld. Multi-day ozone production potential of volatile organic compounds calculated with a tagging approach. *Atmospheric Environment*, 45(24):4082 – 4090, 2011. ISSN 1352-2310. doi:<http://dx.doi.org/10.1016/j.atmosenv.2011.03.040>. URL <http://www.sciencedirect.com/science/article/pii/S1352231011003001>.

S. L. Capps, Y. Hu, and A. G. Russell. Assessing Near-Field and Downwind Impacts of Reactivity-Based Substitutions. *Journal of the Air and Waste Management Association*, 60:316–327, 2010.

W. P. L. Carter. Development of Ozone Reactivity Scales for Volatile Organic Compounds. *Journal of the Air and Waste Management Association*, 44:881–899, 1994.

J. Coates and T. M. Butler. A comparison of chemical mechanisms using tagged ozone production potential (TOPP) analysis. *Atmospheric Chemistry and Physics*, 15(15):8795–8808, 2015. doi:10.5194/acp-15-8795-2015. URL <http://www.atmos-chem-phys.net/15/8795/2015/>.

V. Damian, A. Sandu, M. Damian, F. Potra, and G. R. Carmichael. The kinetic preprocessor KPP-a software environment for solving chemical kinetics. *Computers & Chemical Engineering*, 26(11):1567 – 1579, 2002. ISSN 0098-1354. doi:[http://dx.doi.org/10.1016/S0098-1354\(02\)00128-X](http://dx.doi.org/10.1016/S0098-1354(02)00128-X). URL <http://www.sciencedirect.com/science/article/pii/S009813540200128X>.

R. G. Derwent, M. E. Jenkin, and S. M. Saunders. Photochemical Ozone Creation Potentials for a Large Number of Reactive Hydrocarbons under European Conditions. *Atmospheric Environment*, 30(2):181–199, 1996.

R. G. Derwent, M. E. Jenkin, S. M. Saunders, and M. J. Pilling. Photochemical Ozone Creation Potentials for Organic Compounds in Northwest Europe Calculated with a Master Chemical Mechanism. *Atmospheric Environment*, 32(14/15):2429–2441, 1998.

R. G. Derwent, M. E. Jenkin, M. J. Pilling, W. P. L. Carter, and A. Kaduwela. Reactivity Scales as Comparative Tools for Chemical Mechanisms. *Journal of the Air and Waste Management Association*, 60:914–924, 2010.

G. B. M. Dobson. Origin and distribution of polyatomic molecules in the atmosphere. *Proceedings of the Royal Society London A*, 236(1205):187–193, 1956.

A. M. Dunker, S. Kumar, and P. H. Berzins. A Comparison of Chemical Mechanisms Used In Atmospheric Models. *Atmospheric Environment*, 18(2):311–321, 1984.

EEA. Air quality in Europe - 2013 report. Technical Report 9/2013, European Environmental Agency, 2013.

EEA. Air quality in Europe - 2015 report. Technical Report 5/2015, European Environmental Agency, 2015.

K. M. Emmerson and M. J. Evans. Comparison of tropospheric gas-phase chemistry schemes for use within global models. *Atmospheric Chemistry and Physics*, 9: 1831–1845, 2009.

L. K. Emmons, S. Walters, P. G. Hess, J.-F. Lamarque, G. G. Pfister, D. Fillmore, C. Granier, A. Guenther, D. Kinnison, T. Laepple, J. Orlando, X. Tie, G. Tyndall, C. Wiedinmyer, S. L. Baughcum, and S. Kloster. Description and evaluation of the Model for Ozone and Related chemical Tracers, version 4 (MOZART-4). *Geoscientific Model Development*, 3(1):43–67, 2010. doi:10.5194/gmd-3-43-2010. URL <http://www.geosci-model-dev.net/3/43/2010/>.

A. M. Fiore, D. J. Jacob, J. A. Logan, and J. H. Yin. Long-term trends in ground level ozone over the contiguous United States, 1980-1995. *Journal of Geophysical Research*, 103(D1):1471–1480, 1998.

M. W. Gery, G. Z. Whitten, J. P. Killus, and M. C. Dodge. A photochemical kinetics mechanism for urban and regional scale computer modeling. *Journal of Geophysical Research*, 94(D10):12,925–12,956, 1989.

A. H. Goldstein and I. E. Galbally. Known and unexplored organic constituents in the Earth’s atmosphere. *Environmental Science and Technology*, 41(5):1514–1521, 2007.

W. S. Goliff, W. R. Stockwell, and C. V. Lawson. The regional atmospheric chemistry mechanism, version 2. *Atmospheric Environment*, 68:174 – 185, 2013. ISSN 1352-2310. doi:<http://dx.doi.org/10.1016/j.atmosenv.2012.11.038>. URL <http://www.sciencedirect.com/science/article/pii/S1352231012011065>.

G. Grell, S. Peckham, R. Schmitz, S. McKeen, G. Frost, W. Skamarock, and B. Eder. Fully coupled "online" chemistry within the WRF model. *Atmospheric Environment*, 39(37):6957–6975, 2005.

A. Gross and W. R. Stockwell. Comparison of the EMEP, RADM2 and RACM Mechanisms. *Journal of Atmospheric Chemistry*, 44:151–170, 2003.

P. H. Haynes, C. J. Marks, M. E. McIntyre, T. G. Shephard, and K. P. Shine. On the "Downward Control" of Extratropical Diabatic Circulations by Eddy-Induced Mean Zonal Forces. *Journal of the Atmospheric Sciences*, 48(4):651–687, 1991.

P. Hess and N. Mahowald. Interannual variability in hindcasts of atmospheric chemistry: the role of meteorology. *Atmospheric Chemistry and Physics*, 9:5261–5280, 2009.

H. Hogo and M. Gery. USER'S GUIDE FOR EXECUTING OZIPM-4 (OZONE ISOPLETH PLOTTING WITH OPTIONAL MECHANISMS, VERSION 4) WITH CBM-IV (CARBON-BOND MECHANISMS-IV) OR OPTIONAL MECHANISMS. VOLUME 1. DESCRIPTION OF THE OZONE ISOPLETH PLOTTING PACKAGE. VERSION 4. Technical report, U.S. Environmental Protection Agency, 1989.

L. W. Horowitz, S. Walters, D. L. Mauzerall, L. K. Emmons, P. J. Rasch, C. Granier, X. Tie, J.-F. Lamarque, M. G. Schultz, G. S. Tyndall, J. J. Orlando, and G. P. Brasseur. A global simulation of tropospheric ozone and related tracers: Description and evaluation of MOZART, version 2. *Journal of Geophysical Research: Atmospheres*, 108(D24), 2003. ISSN 2156-2202. doi:10.1029/2002JD002853. URL <http://dx.doi.org/10.1029/2002JD002853>. 4784.

IARC. Outdoor air pollution a leading environmental cause of cancer deaths. https://www.iarc.fr/en/media-centre/iarcnews/pdf/pr221_E.pdf, 2013. [Online; accessed 31-December-2015].

D. J. Jacob and D. A. Winner. Effect of climate change on air quality. *Atmospheric Environment*, 43(1):51 – 63, 2009. ISSN 1352-2310. doi:<http://dx.doi.org/10.1016/j.atmosenv.2008.09.051>. URL <http://www.sciencedirect.com/science/article/pii/S1352231008008571>. Atmospheric Environment - Fifty Years of Endeavour.

M. Jenkin, L. Watson, S. Utembe, and D. Shallcross. A Common Representative Intermediates (CRI) mechanism for VOC degradation. Part 1: Gas phase mechanism development. *Atmospheric Environment*, 42(31):7185 – 7195, 2008. ISSN 1352-2310. doi:<http://dx.doi.org/10.1016/j.atmosenv.2008.07.028>. URL <http://www.sciencedirect.com/science/article/pii/S1352231008006742>.

M. E. Jenkin and K. C. Clemitshaw. Ozone and other secondary photochemical pollutants: Chemical processes governing their formation in the planetary boundary layer. *Atmospheric Environment*, 34(16):2499–2527, 2000.

M. E. Jenkin, S. M. Saunders, and M. J. Pilling. The tropospheric degradation of volatile organic compounds: a protocol for mechanism development. *Atmospheric Environment*, 31(1):81 – 104, 1997. ISSN 1352-2310. doi:[http://dx.doi.org/10.1016/S1352-2310\(96\)00105-7](http://dx.doi.org/10.1016/S1352-2310(96)00105-7). URL <http://www.sciencedirect.com/science/article/pii/S1352231096001057>.

M. E. Jenkin, S. M. Saunders, V. Wagner, and M. J. Pilling. Protocol for the development of the Master Chemical Mechanism, MCM v3 (Part B): tropospheric degradation of aromatic volatile organic compounds. *Atmospheric Chemistry and Physics*, 3(1):181–193, 2003. doi:10.5194/acp-3-181-2003. URL <http://www.atmos-chem-phys.net/3/181/2003/>.

D. E. Kinnison, G. P. Brasseur, S. Walters, R. R. Garcia, D. R. Marsh, F. Sassi, V. L. Harvey, C. E. Randall, L. Emmons, J. F. Lamarque, P. Hess, J. J. Orlando, X. X. Tie, W. Randel, L. L. Pan, A. Gettelman, C. Granier, T. Diehl, U. Niemeier, and A. J. Simmons. Sensitivity of chemical tracers to meteorological parameters in the MOZART-3 chemical transport model. *Journal of Geophysical Research: Atmospheres*, 112(D20), 2007. ISSN 2156-2202. doi:10.1029/2006JD007879. URL <http://dx.doi.org/10.1029/2006JD007879>. D20302.

F. Kirchner and W. R. Stockwell. Effect of peroxy radical reactions on the predicted concentrations of ozone, nitrogenous compounds, and radicals. *Journal of Geophysical Research: Atmospheres*, 101(D15):21007–21022, 1996. ISSN 2156-2202. doi:10.1029/96JD01519. URL <http://dx.doi.org/10.1029/96JD01519>.

F. Kirchner, F. Jenneret, A. Clappier, B. Krüger, H. van den Bergh, and B. Calpini. Total VOC reactivity in the planetary boundary layer 2. A new indicator for determining the sensitivity of the ozone production to VOC and NO_x. *Journal of Geophysical Research*, 106(D3):3095–3110, 2001.

L. I. Kleinman. Seasonal Dependence of Boundary Layer Peroxide Concentration: The Low and High NO_x Regimes. *Journal of Geophysical Research*, 96(D11):20,721–20,733, 1991.

L. I. Kleinman. Low and high NO_x tropospheric photochemistry. *Journal of Geophysical Research*, 99(D8):16,831–16,838, 1994.

L. I. Kleinman. The dependence of tropospheric ozone production rate on ozone precursors. *Atmospheric Environment*, 39(3):575 – 586, 2005. ISSN

1352-2310. doi:<http://dx.doi.org/10.1016/j.atmosenv.2004.08.047>. URL <http://www.sciencedirect.com/science/article/pii/S1352231004008234>.

J.-H. Koo, Y. Wang, T. P. Kurosu, K. Chance, A. Rozanov, A. Richter, S. J. Oltmans, A. M. Thompson, J. W. Hair, M. A. Fenn, A. J. Weinheimer, T. B. Ryerson, S. Solberg, L. G. Huey, J. Liao, J. E. Dibb, J. A. Neuman, J. B. Nowak, R. B. Pierce, M. Natarajan, and J. Al-Saadi. Characteristics of tropospheric ozone depletion events in the Arctic spring: analysis of the ARCTAS, ARCPAC, and ARCIONS measurements and satellite BrO observations. *Atmospheric Chemistry and Physics*, 12:9909–9922, 2012.

D. Kubistin, H. Harder, M. Martinez, M. Rudolf, R. Sander, H. Bozem, G. Eerdeken, H. Fischer, C. Gurk, T. Klüpfel, R. Königstedt, U. Parchatka, C. L. Schiller, A. Stickler, D. Taraborrelli, J. Williams, and J. Lelieveld. Hydroxyl radicals in the tropical troposphere over the Suriname rainforest: comparison of measurements with the box model MECCA. *Atmospheric Chemistry and Physics*, 10(19):9705–9728, 2010. doi:10.5194/acp-10-9705-2010. URL <http://www.atmos-chem-phys.net/10/9705/2010/>.

J. Lelieveld and F. J. Dentener. What controls tropospheric ozone? *Journal of Geophysical Research*, 105(D3):3531–3551, 2000.

X. Li, F. Rohrer, T. Brauers, A. Hofzumahaus, K. Lu, M. Shao, Y. H. Zhang, and A. Wahner. Modeling of HCHO and CHOCHO at a semi-rural site in southern China during the PRIDE-PRD2006 campaign. *Atmospheric Chemistry and Physics*, 14(22):12291–12305, 2014. doi:10.5194/acp-14-12291-2014. URL <http://www.atmos-chem-phys.net/14/12291/2014/>.

C.-Y. C. Lin, D. J. Jacob, and A. M. Fiore. Trends in exceedances of the ozone air quality standard in the continental United States, 1980-1998. *Atmospheric Environment*, 35:3217–3228, 2001.

A. Lourens. *Air quality in the Johannesburg-Pretoria megacity: its regional influence and identification of parameters that could mitigate pollution*. PhD thesis, North-West University, Potchefstroom Campus, 2012.

D. J. Luecken and M. R. Mebust. Technical Challenges Involved in Implementation of VOC Reactivity-Based Control of Ozone. *Environmental Science and Technology*, 42(5):1615–1622, 2008.

W. J. Moxim, H. Levy, and P. S. Kasibhatla. Simulated global tropospheric PAN: Its transport and impact on NO_x. *Journal of Geophysical Research: Atmospheres*,

101(D7):12621–12638, 1996. ISSN 2156-2202. doi:10.1029/96JD00338. URL <http://dx.doi.org/10.1029/96JD00338>.

A. Nölscher, T. Butler, J. Auld, P. Veres, A. Muñoz, D. Taraborrelli, L. Vereecken, J. Lelieveld, and J. Williams. Using total OH reactivity to assess isoprene photooxidation via measurement and model. *Atmospheric Environment*, 89(0): 453–463, 2014. ISSN 1352-2310. doi:10.1016/j.atmosenv.2014.02.024. URL <http://www.sciencedirect.com/science/article/pii/S1352231014001204>.

S. A. Penkett and K. A. Brice. The spring maximum of photo-oxidants in the Northern Hemisphere troposphere. *Nature*, 319:655–657, 1986.

B. Qi, Y. Kanaya, A. Takami, S. Hatakeyama, S. Kato, Y. Sadanaga, H. Tanimoto, and Y. Kajii. Diurnal peroxy radical chemistry at a remote coastal site over the sea of Japan. *Journal of Geophysical Research: Atmospheres*, 112(D17), 2007. ISSN 2156-2202. doi:10.1029/2006JD008236. URL <http://dx.doi.org/10.1029/2006JD008236>. D17306.

A. Rickard, J. Young, M. J. Pilling, M. E. Jenkin, S. Pascoe, and S. M. Saunders. The Master Chemical Mechanism Version MCM v3.2. <http://mcm.leeds.ac.uk/MCMv3.2/>, 2015. [Online; accessed 25-March-2015].

A. Russell and R. Dennis. NARSTO critical review of photochemical models and modeling. *Atmospheric Environment*, 34(12–14):2283 – 2324, 2000. ISSN 1352-2310. doi:[http://dx.doi.org/10.1016/S1352-2310\(99\)00468-9](http://dx.doi.org/10.1016/S1352-2310(99)00468-9). URL <http://www.sciencedirect.com/science/article/pii/S1352231099004689>.

R. Sander, A. Kerkweg, P. Jöckel, and J. Lelieveld. Technical note: The new comprehensive atmospheric chemistry module mecca. *Atmospheric Chemistry and Physics*, 5(2):445–450, 2005. doi:10.5194/acp-5-445-2005. URL <http://www.atmos-chem-phys.net/5/445/2005/>.

A. Sandu, J. Verwer, J. Blom, E. Spee, G. Carmichael, and F. Potra. Benchmarking stiff ode solvers for atmospheric chemistry problems II: Rosenbrock solvers. *Atmospheric Environment*, 31(20):3459 – 3472, 1997a. ISSN 1352-2310. doi:[http://dx.doi.org/10.1016/S1352-2310\(97\)83212-8](http://dx.doi.org/10.1016/S1352-2310(97)83212-8). URL <http://www.sciencedirect.com/science/article/pii/S1352231097832128>.

A. Sandu, J. Verwer, M. V. Loon, G. Carmichael, F. Potra, D. Dabdub, and J. Seinfeld. Benchmarking stiff ode solvers for atmospheric chemistry problems-I. implicit vs explicit . *Atmospheric Environment*, 31(19):3151 – 3166, 1997b. ISSN 1352-2310. doi:[http://dx.doi.org/10.1016/S1352-2310\(97\)00059-9](http://dx.doi.org/10.1016/S1352-2310(97)00059-9). URL <http://www.sciencedirect.com/science/article/pii/S1352231097000599>.

S. M. Saunders, M. E. Jenkin, R. G. Derwent, and M. J. Pilling. Protocol for the development of the Master Chemical Mechanism, MCM v3 (Part A): tropospheric degradation of non-aromatic volatile organic compounds. *Atmospheric Chemistry and Physics*, 3(1):161–180, 2003. doi:10.5194/acp-3-161-2003. URL <http://www.atmos-chem-phys.net/3/161/2003/>.

S. Seefeld and W. Stockwell. First-order sensitivity analysis of models with time-dependent parameters: An application to PAN and ozone. *Atmospheric Environment*, 33(18):2941–2953, 1999.

J. H. Seinfeld and S. N. Pandis. *Atmospheric Chemistry and Physics: From Air Pollution to Climate Change*. John Wiley & Sons Inc, New York, second edition, 2006. ISBN 978-0-471-72018-8.

S. Sillman. The relation between ozone, nox and hydrocarbons in urban and polluted rural environments. *Atmospheric Environment*, 33(12):1821 – 1845, 1999. ISSN 1352-2310. doi:[http://dx.doi.org/10.1016/S1352-2310\(98\)00345-8](http://dx.doi.org/10.1016/S1352-2310(98)00345-8). URL <http://www.sciencedirect.com/science/article/pii/S1352231098003458>.

W. R. Stockwell, P. Middleton, J. S. Chang, and X. Tang. The second generation regional acid deposition model chemical mechanism for regional air quality modeling. *Journal of Geophysical Research: Atmospheres*, 95(D10):16343–16367, 1990. ISSN 2156-2202. doi:10.1029/JD095iD10p16343. URL <http://dx.doi.org/10.1029/JD095iD10p16343>.

W. R. Stockwell, F. Kirchner, M. Kuhn, and S. Seefeld. A new mechanism for regional atmospheric chemistry modeling. *Journal of Geophysical Research: Atmospheres*, 102(D22):25847–25879, 1997. ISSN 2156-2202. doi:10.1029/97JD00849. URL <http://dx.doi.org/10.1029/97JD00849>.

W. R. Stockwell, C. V. Lawson, E. Saunders, and W. S. Goliff. A Review of Tropospheric Atmospheric Chemistry and Gas-Phase Chemical Mechanisms for Air Quality Modeling. *Atmosphere*, 3:1–32, 2012. ISSN 2073-4433.

K. Sudo and M. Takashi. Simulation of tropospheric ozone changes during 1997-1998 El Niño: Meteorological impact on tropospheric photochemistry. *Geophysical Research Letters*, 28(21):4091–4094, 2001.

L. Watson, D. Shallcross, S. Utembe, and M. Jenkin. A Common Representative Intermediates (CRI) mechanism for VOC degradation. Part 2: Gas phase mechanism reduction. *Atmospheric Environment*, 42(31):7196 – 7204, 2008. ISSN 1352-2310. doi:<http://dx.doi.org/10.1016/j.atmosenv.2008.07.034>. URL <http://www.sciencedirect.com/science/article/pii/S1352231008006845>.

World Meteorological Organisation. Scientific Assessment of Ozone Depletion: 2010. Technical Report 516 pp., World Meteorological Organisation, Geneva, Switzerland, March 2011.

Z.-Q. Xie, R. Sander, U. Pöschl, and F. Slemr. Simulation of atmospheric mercury depletion events (AMDEs) during polar springtime using the MECCA box model. *Atmospheric Chemistry and Physics*, 8(23):7165–7180, 2008. doi:10.5194/acp-8-7165-2008. URL <http://www.atmos-chem-phys.net/8/7165/2008/>.

G. Yarwood, S. Rao, M. Yocke, and G. Z. Whitten. Updates to the Carbon Bond Chemical Mechanism: CB05. Technical report, U. S Environmental Protection Agency, 2005.

Chapter 6

Paper 1: A comparison of
chemical mechanisms using tagged
ozone production potential
(TOPP) analysis



A comparison of chemical mechanisms using tagged ozone production potential (TOPP) analysis

J. Coates and T. M. Butler

Institute for Advanced Sustainability Studies, Potsdam, Germany

Correspondence to: J. Coates (jane.coates@iass-potsdam.de)

Received: 10 April 2015 – Published in Atmos. Chem. Phys. Discuss.: 29 April 2015

Revised: 23 July 2015 – Accepted: 24 July 2015 – Published: 10 August 2015

Abstract. Ground-level ozone is a secondary pollutant produced photochemically from reactions of NO_x with peroxy radicals produced during volatile organic compound (VOC) degradation. Chemical transport models use simplified representations of this complex gas-phase chemistry to predict O_3 levels and inform emission control strategies. Accurate representation of O_3 production chemistry is vital for effective prediction. In this study, VOC degradation chemistry in simplified mechanisms is compared to that in the near-explicit Master Chemical Mechanism (MCM) using a box model and by “tagging” all organic degradation products over multi-day runs, thus calculating the tagged ozone production potential (TOPP) for a selection of VOCs representative of urban air masses. Simplified mechanisms that aggregate VOC degradation products instead of aggregating emitted VOCs produce comparable amounts of O_3 from VOC degradation to the MCM. First-day TOPP values are similar across mechanisms for most VOCs, with larger discrepancies arising over the course of the model run. Aromatic and unsaturated aliphatic VOCs have the largest inter-mechanism differences on the first day, while alkanes show largest differences on the second day. Simplified mechanisms break VOCs down into smaller-sized degradation products on the first day faster than the MCM, impacting the total amount of O_3 produced on subsequent days due to secondary chemistry.

gen oxides ($\text{NO}_x = \text{NO} + \text{NO}_2$) in the presence of sunlight (Atkinson, 2000).

Background O_3 concentrations have increased during the last several decades due to the increase of overall global anthropogenic emissions of O_3 precursors (HTAP, 2010). Despite decreases in emissions of O_3 precursors over Europe since 1990, EEA (2014) reports that 98 % of Europe’s urban population are exposed to levels exceeding the WHO air quality guideline of $100 \mu\text{g m}^{-3}$ over an 8 h mean. These exceedances result from local and regional O_3 precursor gas emissions, their intercontinental transport and the non-linear relationship of O_3 concentrations to NO_x and VOC levels (EEA, 2014).

Effective strategies for emission reductions rely on accurate predictions of O_3 concentrations using chemical transport models (CTMs). These predictions require adequate representation of gas-phase chemistry in the chemical mechanism used by the CTM. For reasons of computational efficiency, the chemical mechanisms used by global and regional CTMs must be simpler than the nearly explicit mechanisms which can be used in box modelling studies. This study compares the impacts of different simplification approaches of chemical mechanisms on O_3 production chemistry focusing on the role of VOC degradation products.



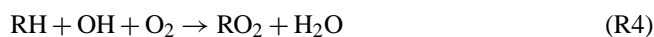
The photochemical cycle (Reactions R1–R3) rapidly produces and destroys O_3 . NO and NO_2 reach a near-steady state via Reactions (R1) and (R2) which is disturbed in two cases. Firstly, via O_3 removal (deposition or Reaction R1 during night-time and near large NO sources) and secondly,

1 Introduction

Ground-level ozone (O_3) is both an air pollutant and a climate forcer that is detrimental to human health and crop growth (Stevenson et al., 2013). O_3 is produced from the reactions of volatile organic compounds (VOCs) and nitro-

when O_3 is produced through VOC– NO_x chemistry (Sillman, 1999).

VOCs (RH) are mainly oxidised in the troposphere by the hydroxyl radical (OH) forming peroxy radicals (RO_2) in the presence of O_2 . For example, Reaction (R4) describes the OH oxidation of alkanes proceeding through abstraction of an H from the alkane. In high- NO_x conditions, typical of urban environments, RO_2 react with NO (Reaction R5) to form alkoxy radicals (RO), which react quickly with O_2 (Reaction R6) producing a hydroperoxy radical (HO_2) and a carbonyl species ($R'CHO$). The secondary chemistry of these first-generation carbon-containing oxidation products is analogous to the sequence of Reactions (R4–R6), producing further HO_2 and RO_2 radicals. Subsequent-generation oxidation products can continue to react, producing HO_2 and RO_2 until they have been completely oxidised to CO_2 and H_2O . Both RO_2 and HO_2 react with NO to produce NO_2 (Reactions R5 and R7) leading to O_3 production via Reactions (R2) and (R3). Thus, the amount of O_3 produced from VOC degradation is related to the number of NO to NO_2 conversions by RO_2 and HO_2 radicals formed during VOC degradation (Atkinson, 2000).

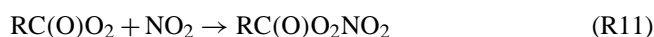


Three atmospheric regimes with respect to O_3 production can be defined (Jenkin and Clemitshaw, 2000). In the NO_x -sensitive regime, VOC concentrations are much higher than those of NO_x , and O_3 production depends on NO_x concentrations. On the other hand, when NO_x concentrations are much higher than those of VOCs (VOC-sensitive regime), VOC concentrations determine the amount of O_3 produced. Finally, the NO_x –VOC-sensitive regime produces maximal O_3 and is controlled by both VOC and NO_x concentrations.

These atmospheric regimes remove radicals through distinct mechanisms (Kleinman, 1991). In the NO_x -sensitive regime, radical concentrations are high relative to NO_x leading to radical removal by radical combination (Reaction R8) and bimolecular destruction (Reaction R9) (Kleinman, 1994).



However, in the VOC-sensitive regime, radicals are removed by reacting with NO_2 leading to nitric acid (HNO_3) (Reaction R10) and PAN species (Reaction R11).



The NO_x –VOC-sensitive regime has no dominant radical removal mechanism as radical and NO_x amounts are compara-

ble. This chemistry results in O_3 concentrations being a non-linear function of NO_x and VOC concentrations.

Individual VOCs impact O_3 production differently through their diverse reaction rates and degradation pathways. These impacts can be quantified using ozone production potentials (OPPs), which can be calculated through incremental reactivity (IR) studies using photochemical models. In IR studies, VOC concentrations are changed by a known increment and the change in O_3 production is compared to that of a standard VOC mixture. Examples of IR scales are the maximum incremental reactivity (MIR) and maximum ozone incremental reactivity (MOIR) scales in Carter (1994), as well as the photochemical ozone creation potential (POCP) scale of Derwent et al. (1996, 1998). The MIR, MOIR and POCP scales were calculated under different NO_x conditions, thus calculating OPPs in different atmospheric regimes.

Butler et al. (2011) calculate the maximum potential of a number of VOCs to produce O_3 by using NO_x conditions inducing NO_x –VOC-sensitive chemistry over multi-day scenarios using a “tagging” approach – the tagged ozone production potential (TOPP). Tagging involves labelling all organic degradation products produced during VOC degradation with the name of the emitted VOCs. Tagging enables the attribution of O_3 production from VOC degradation products back to the emitted VOCs, thus providing detailed insight into VOC degradation chemistry. Butler et al. (2011), using a near-explicit chemical mechanism, showed that some VOCs, such as alkanes, produce maximum O_3 on the second day of the model run; in contrast to unsaturated aliphatic and aromatic VOCs which produce maximum O_3 on the first day. In this study, the tagging approach of Butler et al. (2011) is applied to several chemical mechanisms of reduced complexity, using conditions of maximum O_3 production (NO_x –VOC-sensitive regime), to compare the effects of different representations of VOC degradation chemistry on O_3 production in the different chemical mechanisms.

A near-explicit mechanism, such as the Master Chemical Mechanism (MCM) (Jenkin et al., 2003; Saunders et al., 2003; Bloss et al., 2005), includes detailed degradation chemistry making the MCM ideal as a reference for comparing chemical mechanisms. Reduced mechanisms generally take two approaches to simplifying the representation of VOC degradation chemistry: lumped-structure approaches and lumped-molecule approaches (Dodge, 2000).

Lumped-structure mechanisms speciate VOCs by the carbon bonds of the emitted VOCs (e.g. the Carbon Bond mechanisms, CBM-IV (Gery et al., 1989) and CB05 (Yarwood et al., 2005)). Lumped-molecule mechanisms represent VOCs explicitly or by aggregating (lumping) many VOCs into a single mechanism species. Mechanism species may lump VOCs by functionality (MOdel for Ozone and Related chemical Tracers, MOZART-4, Emmons et al., 2010) or OH reactivity (Regional Acid Deposition Model, RADM2 (Stockwell et al., 1990), Regional Atmospheric Chemistry

Mechanism, RACM (Stockwell et al., 1997) and RACM2 (Goliff et al., 2013)). The Common Representative Intermediates mechanism (CRI) lumps the degradation products of VOCs rather than the emitted VOCs (Jenkin et al., 2008).

Many comparison studies of chemical mechanisms consider modelled time series of O₃ concentrations over varying VOC and NO_x concentrations. Examples are Dunker et al. (1984), Kuhn et al. (1998) and Emmerson and Evans (2009). The largest discrepancies between the time series of O₃ concentrations in different mechanisms from these studies arise when modelling urban rather than rural conditions and are attributed to the treatment of radical production, organic nitrate and night-time chemistry. Emmerson and Evans (2009) also compare the inorganic gas-phase chemistry of different chemical mechanisms; differences in inorganic chemistry arise from inconsistencies between IUPAC and JPL reaction rate constants.

Mechanisms have also been compared using OPP scales. OPPs are a useful comparison tool as they relate O₃ production to a single value. Derwent et al. (2010) compared the near-explicit MCM v3.1 and SAPRC-07 mechanisms using first-day POCP values calculated under VOC-sensitive conditions. The POCP values were comparable between the mechanisms. Butler et al. (2011) compared first-day TOPP values to the corresponding published MIR, MOIR and POCP values. TOPP values were most comparable to MOIR and POCP values due to the similarity of the chemical regimes used in their calculation.

In this study, we compare TOPP values of VOCs using a number of mechanisms to those calculated with the MCM v3.2, under standardised conditions which maximise O₃ production. Differences in O₃ production are explained by the differing treatments of secondary VOC degradation in these mechanisms.

2 Methodology

2.1 Chemical mechanisms

The nine chemical mechanisms compared in this study are outlined in Table 1 with a brief summary below. We used a subset of each chemical mechanism containing all the reactions needed to fully describe the degradation of the VOCs in Table 2. The reduced mechanisms in this study were chosen as they are commonly used in 3-D models and apply different approaches to representing secondary VOC chemistry. The recent review by Baklanov et al. (2014) shows that each chemical mechanism used in this study are actively used by modelling groups.

The MCM (Jenkin et al., 1997, 2003; Saunders et al., 2003; Bloss et al., 2005; Rickard et al., 2015) is a near-explicit mechanism which describes the degradation of 125 primary VOCs. The MCM v3.2 is the reference mechanism in this study due to its level of detail (16 349 organic reac-

tions). Despite this level of detail, the MCM had difficulties in reproducing the results of chamber study experiments involving aromatic VOCs (Bloss et al., 2005).

The CRI (Jenkin et al., 2008) is a reduced chemical mechanism with 1145 organic reactions describing the oxidation of the same primary VOCs as the MCM v3.1 (12 691 organic reactions). VOC degradation in the CRI is simplified by lumping the degradation products of many VOCs into mechanism species whose overall O₃ production reflects that of the MCM v3.1. The CRI v2 is available in more than one reduced variant, described in Watson et al. (2008). We used a subset of the full version of the CRI v2 (<http://mcm.leeds.ac.uk/CRI>). Differences in O₃ production between the CRI v2 and MCM v3.2 may be due to changes in the MCM versions rather than the CRI reduction techniques, hence the MCM v3.1 is also included in this study.

MOZART-4 represents global tropospheric and stratospheric chemistry (Emmons et al., 2010). Explicit species exist for methane, ethane, propane, ethene, propene, isoprene and α -pinene. All other VOCs are represented by lumped species determined by the functionality of the VOCs. Tropospheric chemistry is described by 145 organic reactions in MOZART-4.

RADM2 (Stockwell et al., 1990) describes regional-scale atmospheric chemistry using 145 organic reactions with explicit species representing methane, ethane, ethene and isoprene. All other VOCs are assigned to lumped species based on OH reactivity and molecular weight. RADM2 was updated to RACM (Stockwell et al., 1997) with more explicit and lumped species representing VOCs as well as revised chemistry (193 organic reactions). RACM2 is the updated RACM version (Goliff et al., 2013) with substantial updates to the chemistry, including more lumped and explicit species representing emitted VOCs (315 organic reactions).

CBM-IV (Gery et al., 1989) uses 46 organic reactions to simulate polluted urban conditions and represents ethene, formaldehyde and isoprene explicitly while all other emitted VOCs are lumped by their carbon bond types. All primary VOCs were assigned to lumped species in CBM-IV as described in Hogo and Gery (1989). For example, the mechanism species PAR represents the C–C bond. Pentane, having five carbon atoms, is represented as 5 PAR. A pentane mixing ratio of 1200 pptv is assigned to 6000 (= 1200 \times 5) pptv of PAR in CBM-IV. CBM-IV was updated to CB05 (Yarwood et al., 2005) by including further explicit species representing methane, ethane and acetaldehyde, and has 99 organic reactions. Other updates include revised allocation of primary VOCs and updated rate constants.

2.2 Model set-up

The modelling approach and set-up follows the original TOPP study of Butler et al. (2011). The approach is summarised here; further details can be found in the Supplement and in Butler et al. (2011). We use the MECCA box model,

Table 1. The chemical mechanisms used in the study are shown here. MCM v3.2 is the reference mechanism. The number of organic species and reactions needed to fully oxidise the VOCs in Table 2 for each mechanism are also included.

| Chemical mechanism | Number of organic species | Number of organic reactions | Type of lumping | Reference | Recent study |
|--------------------|---------------------------|-----------------------------|----------------------|-------------------------|-----------------------|
| MCM v3.2 | 1884 | 5621 | No lumping | Rickard et al. (2015) | Koss et al. (2015) |
| MCM v3.1 | 1677 | 4862 | No lumping | Jenkin et al. (1997) | Lidster et al. (2014) |
| | | | | Saunders et al. (2003) | |
| | | | | Jenkin et al. (2003) | |
| | | | | Bloss et al. (2005) | |
| CRI v2 | 189 | 559 | Lumped intermediates | Jenkin et al. (2008) | Derwent et al. (2015) |
| MOZART-4 | 61 | 135 | Lumped molecule | Emmons et al. (2010) | Hou et al. (2015) |
| RADM2 | 42 | 105 | Lumped molecule | Stockwell et al. (1990) | Li et al. (2014) |
| RACM | 51 | 152 | Lumped molecule | Stockwell et al. (1997) | Ahmadov et al. (2015) |
| RACM2 | 92 | 244 | Lumped molecule | Goliff et al. (2013) | Goliff et al. (2015) |
| CBM-IV | 19 | 47 | Lumped structure | Gery et al. (1989) | Foster et al. (2014) |
| CB05 | 33 | 86 | Lumped structure | Yarwood et al. (2005) | Dunker et al. (2015) |

originally described by Sander et al. (2005), and as subsequently modified by Butler et al. (2011) to include MCM chemistry. In this study, the model is run under conditions representative of 34° N at the equinox (broadly representative of the city of Los Angeles, USA).

Maximum O₃ production is achieved in each model run by balancing the chemical source of radicals and NO_x at each time step by emitting the appropriate amount of NO. These NO_x conditions induce NO_x–VOC-sensitive chemistry. Ambient NO_x conditions are not required as this study calculates the maximum potential of VOCs to produce O₃. Future work should verify the extent to which the maximum potential of VOCs to produce O₃ is reached under ambient NO_x conditions.

VOCs typical of Los Angeles and their initial mixing ratios are taken from Baker et al. (2008), listed in Table 2. Following Butler et al. (2011), the associated emissions required to keep the initial mixing ratios of each VOC constant until noon of the first day were determined for the MCM v3.2. These emissions are subsequently used for each mechanism, ensuring the amount of each VOC emitted was the same in every model run. Methane (CH₄) was fixed at 1.8 ppmv while CO and O₃ were initialised at 200 and 40 ppbv and then allowed to evolve freely.

The VOCs used in this study are assigned to mechanism species following the recommendations from the literature of each mechanism (Table 1), the representation of each VOC in the mechanisms is found in Table 2. Emissions of lumped species are weighted by the carbon number of the mechanism species ensuring the total amount of emitted reactive carbon was the same in each model run.

The MECCA box model is based upon the Kinetic Pre-Processor (KPP) (Damian et al., 2002). Hence, all chemical mechanisms were adapted into modularised KPP format. The inorganic gas-phase chemistry described in the MCM v3.2 was used in each run to remove any differences between

treatments of inorganic chemistry in each mechanism. Thus, differences between the O₃ produced by the mechanisms are due to the treatment of organic degradation chemistry.

The MCM v3.2 approach to photolysis, dry deposition of VOC oxidation intermediates and RO₂–RO₂ reactions was used for each mechanism; details of these adaptations can be found in the Supplement. Some mechanisms include reactions which are only important in the stratosphere or free troposphere. For example, PAN photolysis is only important in the free troposphere (Harwood et al., 2003) and was removed from MOZART-4, RACM2 and CB05 for the purpose of the study, as this study considers processes occurring within the planetary boundary layer.

2.3 Tagged ozone production potential (TOPP)

This section summarises the tagging approach described in Butler et al. (2011) which is applied in this study.

2.3.1 O_x family and tagging approach

O₃ production and loss is dominated by rapid photochemical cycles, such as Reactions (R1)–(R3). The effects of rapid production and loss cycles can be removed by using chemical families that include rapidly inter-converting species. In this study, we define the O_x family to include O₃, O(³P), O(¹D), NO₂ and other species involved in fast cycling with NO₂, such as HO₂NO₂ and PAN species. Thus, production of O_x can be used as a proxy for production of O₃.

The tagging approach follows the degradation of emitted VOCs through all possible pathways by labelling every organic degradation product with the name of the emitted VOCs. Thus, each emitted VOC effectively has its own set of degradation reactions. Butler et al. (2011) showed that O_x production can be attributed to the VOCs by following the tags of each VOC.

Table 2. Non-methane volatile organic compounds (NMVOCs) present in Los Angeles. Mixing ratios are taken from Baker et al. (2008) and their representation in each chemical mechanism. The representation of the VOCs in each mechanism is based upon the recommendations of the literature for each mechanism (Table 1).

| NMVOCs | Mixing ratio (pptv) | MCM v3.1, v3.2, CRI v2 | MOZART-4 | RADM2 | RACM | RACM2 | CBM-IV | CB05 |
|-----------------|---------------------|------------------------|----------|-------|------|-------|-------------------|--------------|
| Alkanes | | | | | | | | |
| Ethane | 6610 | C2H6 | C2H6 | ETH | ETH | ETH | 0.4 PAR | ETHA |
| Propane | 6050 | C3H8 | C3H8 | HC3 | HC3 | HC3 | 1.5 PAR | 1.5 PAR |
| Butane | 2340 | NC4H10 | BIGALK | HC3 | HC3 | HC3 | 4 PAR | 4 PAR |
| 2-Methylpropane | 1240 | IC4H10 | BIGALK | HC3 | HC3 | HC3 | 4 PAR | 4 PAR |
| Pentane | 1200 | NC5H12 | BIGALK | HC5 | HC5 | HC5 | 5 PAR | 5 PAR |
| 2-Methylbutane | 2790 | IC5H12 | BIGALK | HC5 | HC5 | HC5 | 5 PAR | 5 PAR |
| Hexane | 390 | NC6H14 | BIGALK | HC5 | HC5 | HC5 | 6 PAR | 6 PAR |
| Heptane | 160 | NC7H16 | BIGALK | HC5 | HC5 | HC5 | 7 PAR | 7 PAR |
| Octane | 80 | NC8H18 | BIGALK | HC8 | HC8 | HC8 | 8 PAR | 8 PAR |
| Alkenes | | | | | | | | |
| Ethene | 2430 | C2H4 | C2H4 | OL2 | ETE | ETE | ETH | ETH |
| Propene | 490 | C3H6 | C3H6 | OLT | OLT | OLT | OLE + PAR | OLE + PAR |
| Butene | 65 | BUT1ENE | BIGENE | OLT | OLT | OLT | OLE + 2 PAR | OLE + 2 PAR |
| 2-Methylpropene | 130 | MEPROPENE | BIGENE | OLI | OLI | OLI | PAR + FORM + ALD2 | FORM + 3 PAR |
| Isoprene | 270 | C5H8 | ISOP | ISO | ISO | ISO | ISOP | ISOP |
| Aromatics | | | | | | | | |
| Benzene | 480 | BENZENE | TOLUENE | TOL | TOL | BEN | PAR | PAR |
| Toluene | 1380 | TOLUENE | TOLUENE | TOL | TOL | TOL | TOL | TOL |
| m-Xylene | 410 | MXYL | TOLUENE | XYL | XYL | XYM | XYL | XYL |
| p-Xylene | 210 | PXYL | TOLUENE | XYL | XYL | XYP | XYL | XYL |
| o-Xylene | 200 | OXYL | TOLUENE | XYL | XYL | XYO | XYL | XYL |
| Ethylbenzene | 210 | EBENZ | TOLUENE | TOL | TOL | TOL | TOL + PAR | TOL + PAR |

O_x production from lumped-mechanism species are re-assigned to the VOCs of Table 2 by scaling the O_x production of the mechanism species by the fractional contribution of each represented VOC. For example, TOL in RACM2 represents toluene and ethylbenzene with fractional contributions of 0.87 and 0.13 to TOL emissions. Scaling the O_x production from TOL by these factors gives the O_x production from toluene and ethylbenzene in RACM2.

Many reduced mechanisms use an operator species as a surrogate for RO_2 during VOC degradation enabling these mechanisms to produce O_x while minimising the number of RO_2 species represented. O_x production from operator species is assigned as O_x production from the organic degradation species producing the operator. This allocation technique is also used to assign O_x production from HO_2 via Reaction (R7).

2.3.2 Definition of TOPP

Attributing O_x production to individual VOCs using the tagging approach is the basis for calculating the TOPP of a VOC, which is defined as the number of O_x molecules produced per emitted molecule of VOC. The TOPP value of

a VOC that is not represented explicitly in a chemical mechanism is calculated by multiplying the TOPP value of the mechanism species representing the VOCs by the ratio of the carbon numbers of the VOCs to the mechanism species. For example, CB05 represents hexane as 6 PAR, so the TOPP value of hexane in the CB05 is 6 times the TOPP of PAR. MOZART-4 represents hexane with the five carbon species BIGALK. Thus, hexane emissions are represented molecule for molecule as $\frac{6}{5}$ of the equivalent number of molecules of BIGALK, and the TOPP value of hexane in MOZART-4 is calculated by multiplying the TOPP value of BIGALK by $\frac{6}{5}$.

3 Results

3.1 Ozone time series and O_x production budgets

Figure 1 shows the time series of O_3 mixing ratios obtained with each mechanism. There is an 8 ppbv difference in O_3 mixing ratios on the first day between RADM2, which has the highest O_3 , and RACM2, which has the lowest O_3 mixing ratios when not considering the outlier time series of RACM. The difference between RADM2 and RACM, the low outlier, was 21 ppbv on the first day. The O_3 mixing ratios in

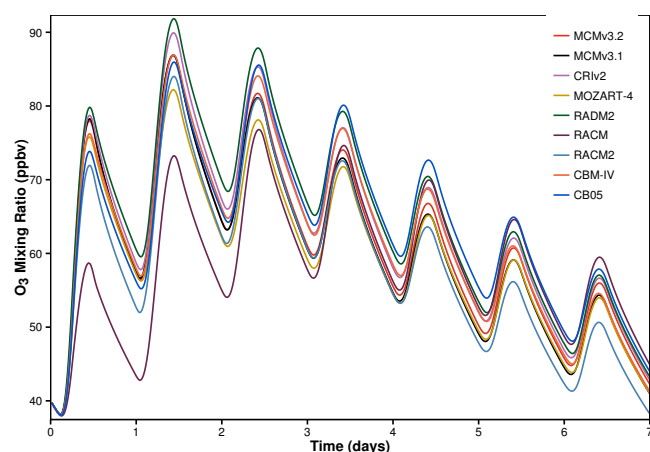


Figure 1. Time series of O_3 mixing ratios obtained using each mechanism.

the CRI v2 are larger than those in the MCM v3.1, which is similar to the results in Jenkin et al. (2008) where the O_3 mixing ratios of the CRI v2 and MCM v3.1 are compared over a 5-day period.

The O_3 mixing ratios in Fig. 1 are influenced by the approaches used in developing the chemical mechanisms and not a function of the explicitness of the chemical mechanism. For example, the O_3 mixing ratios obtained using the Carbon Bond mechanisms (CBM-IV and CB05) compare well with the MCM despite both Carbon Bond mechanisms having $\sim 1\%$ of the number of reactions in the MCM v3.2. Also, the O_3 mixing ratios from RACM2 and RADM2 show similar absolute differences from that of the MCM despite RACM2 having more than double the number of reactions of RADM2.

The day-time O_x production budgets allocated to individual VOCs for each mechanism are shown in Fig. 2. The relationships between O_3 mixing ratios in Fig. 1 are mirrored in Fig. 2 where mechanisms producing high amounts of O_x also have high O_3 mixing ratios. The conditions in the box model lead to a daily maximum of OH that increases with each day leading to an increase on each day in both the reaction rate of the OH oxidation of CH_4 and the daily contribution of CH_4 to O_x production.

The first-day mixing ratios of O_3 in RACM are lower than other mechanisms due to a lack of O_x production from aromatic VOCs on the first day in RACM (Fig. 2). Aromatic degradation chemistry in RACM results in net loss of O_x on the first day, described later in Sect. 3.2.1.

RADM2 is the only reduced mechanism that produces higher O_3 mixing ratios than the more detailed mechanisms (MCM v3.2, MCM v3.1 and CRI v2). Higher mixing ratios of O_3 in RADM2 are produced due to increased O_x production from propane compared to the MCM v3.2; on the first day, the O_x production from propane in RADM2 is triple that of the MCM v3.2 (Fig. 2). Propane is represented as HC3 in

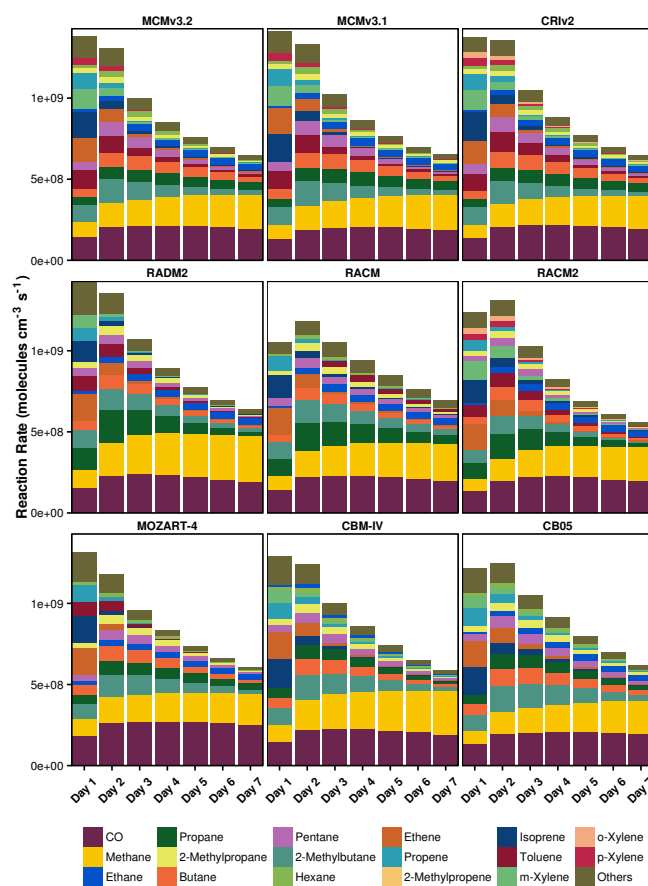


Figure 2. Day-time O_x production budgets in each mechanism allocated to individual VOCs.

RADM2 (Stockwell et al., 1990) and the degradation of HC3 has a lower yield of the less-reactive ketones compared to the MCM. The further degradation of ketones hinders O_x production due to the low OH reactivity and photolysis rate of ketones. Secondary degradation of HC3 proceeds through the degradation of acetaldehyde (CH_3CHO) propagating O_x production through the reactions of CH_3CO_3 and CH_3O_2 with NO. Thus, the lower ketone yields lead to increased O_x production from propane degradation in RADM2 compared to the MCM v3.2.

3.2 Time-dependent O_x production

Time series of daily TOPP values for each VOC are presented in Fig. 3 and the cumulative TOPP values at the end of the model run obtained for each VOC using each of the mechanisms, normalised by the number of atoms of C in each VOC are presented in Table 3. In the MCM and CRI v2, the cumulative TOPP values obtained for each VOC show that by the end of the model run, larger alkanes have produced more O_x per unit of reactive C than alkenes or aromatic VOCs. By the end of the runs using the lumped-structure mechanisms (CBM-IV and CB05), alkanes produce similar

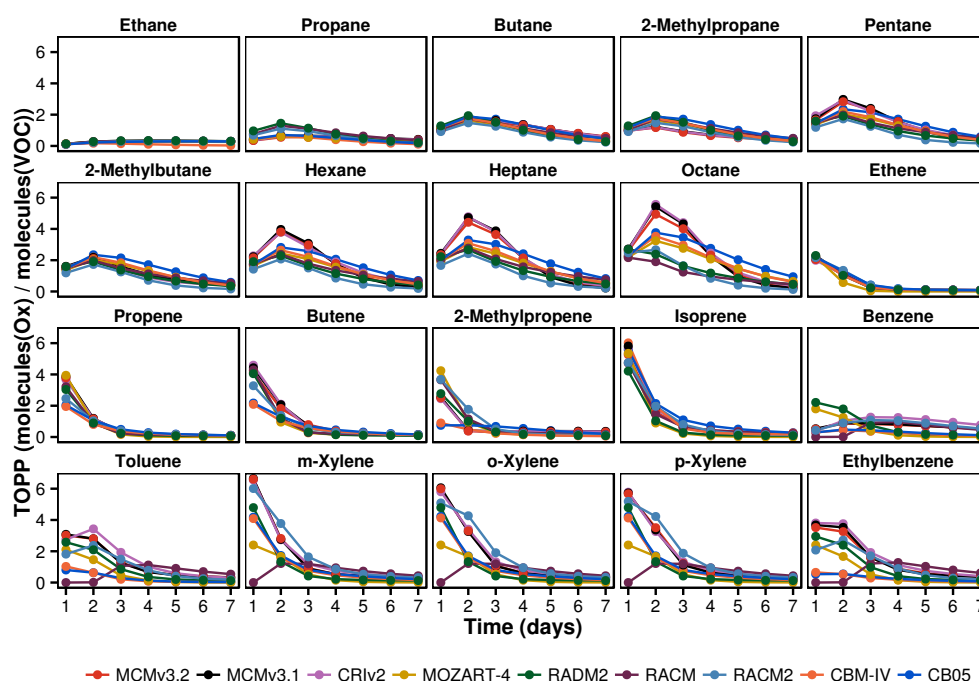


Figure 3. TOPP value time series using each mechanism for each VOC.

Table 3. Cumulative TOPP values at the end of the model run for all VOCs with each mechanism, normalised by the number of C atoms in each VOC.

| NMVOCS | MCM v3.2 | MCM v3.1 | CRIV2 | MOZART-4 | RADM2 | RACM | RACM2 | CBM-IV | CB05 |
|-----------------|----------|----------|-------|----------|-------|------|-------|--------|------|
| Alkanes | | | | | | | | | |
| Ethane | 0.9 | 1.0 | 0.9 | 0.9 | 1.0 | 1.0 | 0.9 | 0.3 | 0.9 |
| Propane | 1.1 | 1.2 | 1.2 | 1.1 | 1.8 | 1.8 | 1.4 | 0.9 | 1.0 |
| Butane | 2.0 | 2.0 | 2.0 | 1.7 | 1.8 | 1.8 | 1.4 | 1.7 | 2.1 |
| 2-Methylpropane | 1.3 | 1.3 | 1.3 | 1.7 | 1.8 | 1.8 | 1.4 | 1.7 | 2.1 |
| Pentane | 2.1 | 2.1 | 2.2 | 1.7 | 1.5 | 1.6 | 1.1 | 1.7 | 2.1 |
| 2-Methylbutane | 1.6 | 1.6 | 1.5 | 1.7 | 1.5 | 1.6 | 1.1 | 1.7 | 2.1 |
| Hexane | 2.1 | 2.1 | 2.2 | 1.7 | 1.5 | 1.6 | 1.1 | 1.7 | 2.1 |
| Heptane | 2.0 | 2.1 | 2.2 | 1.7 | 1.5 | 1.6 | 1.1 | 1.7 | 2.1 |
| Octane | 2.0 | 2.0 | 2.2 | 1.7 | 1.2 | 1.0 | 1.0 | 1.7 | 2.1 |
| Alkenes | | | | | | | | | |
| Ethene | 1.9 | 1.9 | 1.9 | 1.4 | 2.0 | 2.0 | 2.2 | 1.9 | 2.2 |
| Propene | 1.9 | 2.0 | 1.9 | 1.7 | 1.5 | 1.6 | 1.5 | 1.2 | 1.4 |
| Butene | 1.9 | 2.0 | 2.0 | 1.5 | 1.5 | 1.6 | 1.5 | 0.8 | 0.9 |
| 2-Methylpropene | 1.1 | 1.2 | 1.2 | 1.5 | 1.1 | 1.5 | 1.6 | 0.5 | 0.5 |
| Isoprene | 1.8 | 1.8 | 1.8 | 1.3 | 1.2 | 1.6 | 1.7 | 1.9 | 2.1 |
| Aromatics | | | | | | | | | |
| Benzene | 0.8 | 0.8 | 1.1 | 0.6 | 0.9 | 0.6 | 0.9 | 0.3 | 0.3 |
| Toluene | 1.3 | 1.3 | 1.5 | 0.6 | 0.9 | 0.6 | 1.0 | 0.3 | 0.3 |
| m-Xylene | 1.5 | 1.5 | 1.6 | 0.6 | 0.9 | 0.6 | 1.7 | 0.9 | 1.0 |
| p-Xylene | 1.5 | 1.5 | 1.6 | 0.6 | 0.9 | 0.6 | 1.7 | 0.9 | 1.0 |
| o-Xylene | 1.5 | 1.5 | 1.6 | 0.6 | 0.9 | 0.6 | 1.7 | 0.9 | 1.0 |
| Ethylbenzene | 1.3 | 1.4 | 1.5 | 0.6 | 0.9 | 0.6 | 1.0 | 0.2 | 0.3 |

amounts of O_x per reactive C, while aromatic VOCs and some alkenes produce less O_x per reactive C than the MCM. However, in lumped-molecule mechanisms (MOZART-4, RADM2, RACM, RACM2), practically all VOCs produce less O_x per reactive C than the MCM by the end of the run. This lower efficiency of O_x production from many individual VOCs in lumped-molecule and lumped-structure mechanisms would lead to an underestimation of O_3 levels downwind of an emission source, and a smaller contribution to background O_3 when using lumped-molecule and lumped-structure mechanisms.

The lumped-intermediate mechanism (CRI v2) produces the most similar O_x to the MCM v3.2 for each VOC, seen in Fig. 3 and Table 3. Higher variability in the time-dependent O_x production is evident for VOCs represented by lumped-mechanism species. For example, 2-methylpropene, represented in the reduced mechanisms by a variety of lumped species, has a higher spread in time-dependent O_x production than ethene, which is explicitly represented in each mechanism.

In general, the largest differences in O_x produced by aromatic and alkene species are on the first day of the simulations, while the largest inter-mechanism differences in O_x produced by alkanes are on the second and third days of the simulations. The reasons for these differences in behaviour will be explored in Sect. 3.2.1, which examines differences in first day O_x production between the chemical mechanisms, and Sect. 3.2.2, which examines the differences in O_x production on subsequent days.

3.2.1 First-day ozone production

The first-day TOPP values of each VOC from each mechanism, representing O_3 production from freshly emitted VOCs near their source region, are compared to those obtained with the MCM v3.2 in Fig. 4. The root mean square error (RMSE) of all first-day TOPP values in each mechanism relative to those in the MCM v3.2 are also included in Fig. 4. The RMSE value of the CRI v2 shows that first-day O_x production from practically all the individual VOC matches that in the MCM v3.2. All other reduced mechanisms have much larger RMSE values indicating that the first-day O_x production from the majority of the VOCs differs from that in the MCM v3.2.

The reduced complexity of reduced mechanisms means that aromatic VOCs are typically represented by one or two mechanism species leading to differences in O_x production of the actual VOCs compared to the MCM v3.2. For example, all aromatic VOCs in MOZART-4 are represented as toluene, thus less-reactive aromatic VOCs, such as benzene, produce higher O_x whilst more-reactive aromatic VOCs, such as the xylenes, produce less O_x in MOZART-4 than the MCM v3.2. RACM2 includes explicit species representing benzene, toluene and each xylene resulting in O_x production

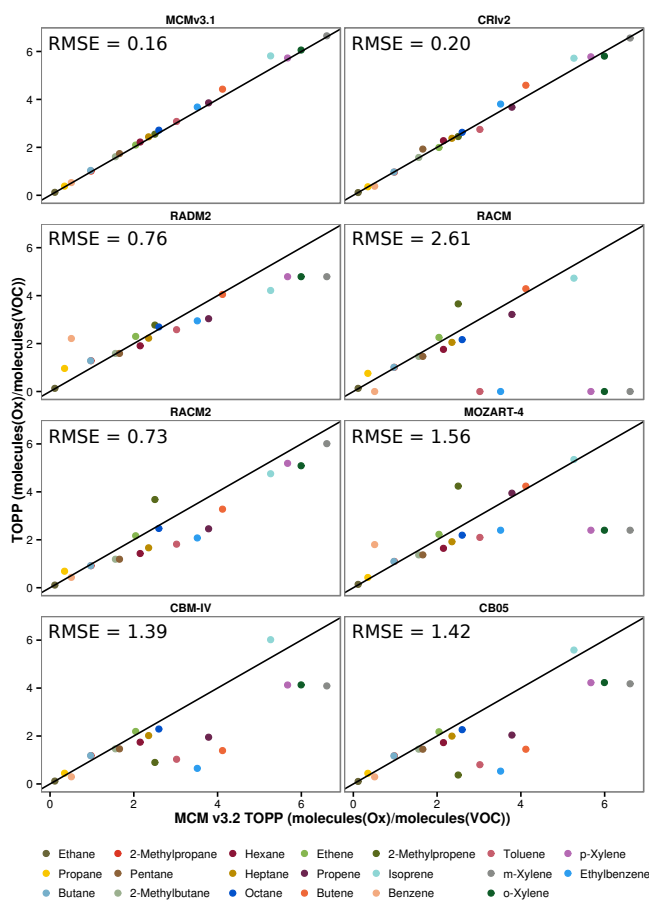


Figure 4. The first-day TOPP values for each VOC calculated using MCM v3.2 and the corresponding values in each mechanism. The root mean square error (RMSE) of each set of TOPP values is also displayed. The black line is the 1 : 1 line.

that is the most similar to the MCM v3.2 than other reduced mechanisms.

Figure 3 shows a high spread in O_x production from aromatic VOCs on the first day indicating that aromatic degradation is treated differently between mechanisms. Toluene degradation is examined in more detail by comparing the reactions contributing to O_x production and loss in each mechanism, shown in Fig. 5. These reactions are determined by following the “toluene” tags in the tagged version of each mechanism.

Toluene degradation in RACM includes several reactions consuming O_x that are not present in the MCM, resulting in net loss of O_x on the first 2 days. Ozonolysis of the cresol OH adduct mechanism species, ADDC, contributes significantly to O_x loss in RACM. This reaction was included in RACM due to improved cresol product yields when comparing RACM predictions with experimental data (Stockwell et al., 1997). Other mechanisms that include cresol OH adduct species do not include ozonolysis and these reactions are not included in the updated RACM2.

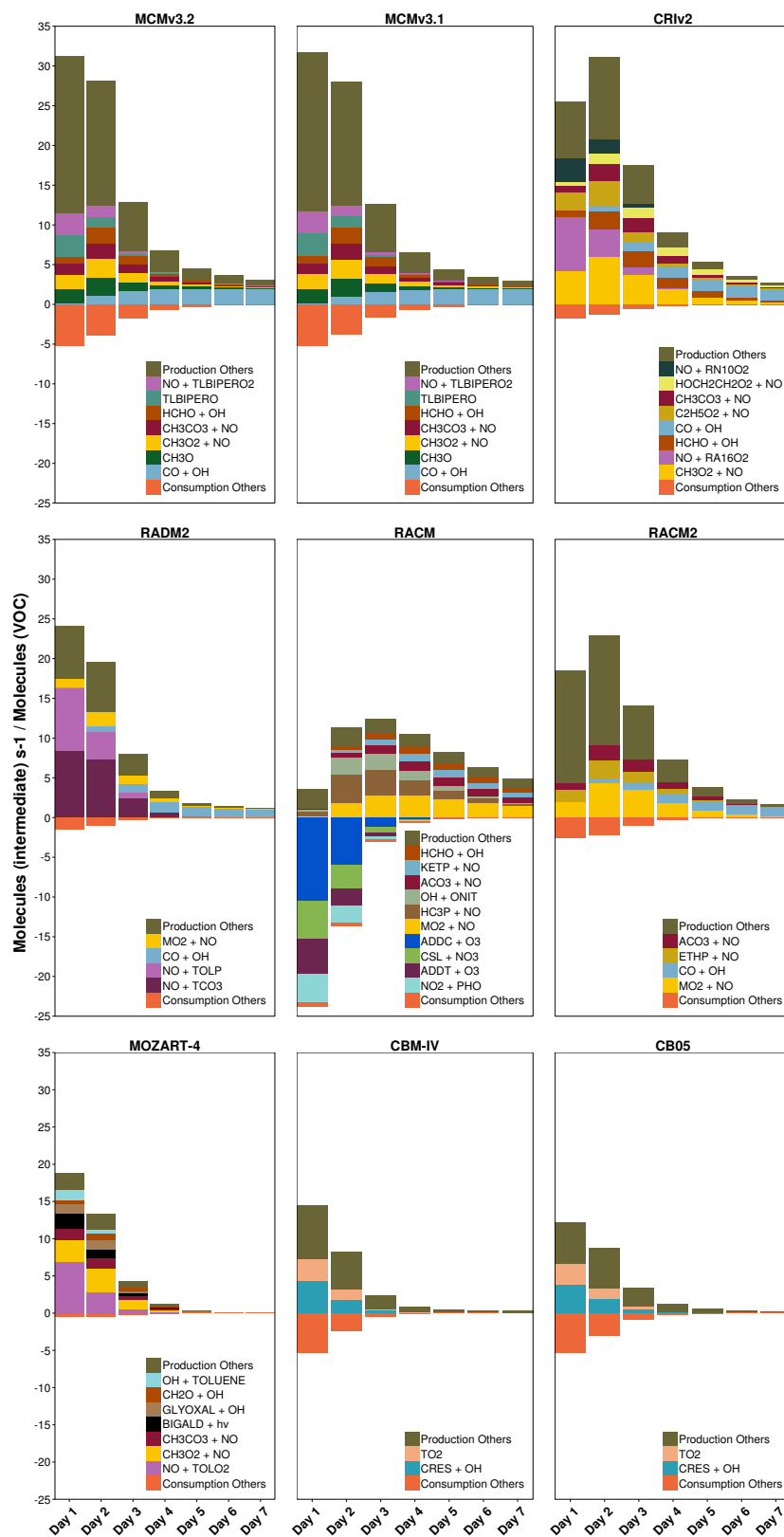


Figure 5. Day-time O_x production and loss budgets allocated to the responsible reactions during toluene degradation in all mechanisms. These reactions are presented using the species defined in each mechanism in Table 1.

The total O_x produced on the first day during toluene degradation in each reduced mechanism is less than that in the MCM v3.2 (Fig. 5). Less O_x is produced in all reduced mechanisms due to a faster breakdown of the VOCs into smaller fragments than the MCM, described later in Sect. 3.3. Moreover, in CBM-IV and CB05, less O_x is produced during toluene degradation as reactions of the toluene degradation products CH_3O_2 and CO do not contribute to the O_x production budgets, which is not the case in any other mechanism (Fig. 5).

Maximum O_x production from toluene degradation in CRI v2 and RACM2 is reached on the second day in contrast to the MCM v3.2 which produces peak O_x on the first day. The second-day maximum of O_x production in CRI v2 and RACM2 from toluene degradation results from more efficient production of unsaturated dicarbonyls than the MCM v3.2. The degradation of unsaturated dicarbonyls produces peroxy radicals such as $C_2H_5O_2$ which promote O_x production via reactions with NO.

Unsaturated aliphatic VOCs generally produce similar amounts of O_x between mechanisms, especially explicitly represented VOCs, such as ethene and isoprene. On the other hand, unsaturated aliphatic VOCs that are not explicitly represented produce differing amounts of O_x between mechanisms (Fig. 3). For example, the O_x produced during 2-methylpropene degradation varies between mechanisms; differing rate constants of initial oxidation reactions and non-realistic secondary chemistry lead to these differences; further details are found in the Supplement.

Non-explicit representations of aromatic and unsaturated aliphatic VOCs coupled with differing degradation chemistry and a faster breakdown into smaller-size degradation products results in different O_x production in lumped-molecule and lumped-structure mechanisms compared to the MCM v3.2.

3.2.2 Ozone production on subsequent days

Alkane degradation in CRI v2 and both MCMs produces a second-day maximum in O_x that increases with alkane carbon number (Fig. 3). The increase in O_x production on the second day is reproduced for each alkane by the reduced mechanisms, except octane in RADM2, RACM and RACM2. However, larger alkanes produce less O_x than the MCM on the second day in all lumped-molecule and lumped-structure mechanisms.

The lumped-molecule mechanisms (MOZART-4, RADM2, RACM and RACM2) represent many alkanes by mechanism species which may lead to unrepresentative secondary chemistry for alkane degradation. For example, 3 times more O_x is produced during the degradation of propane in RADM2 than the MCM v3.2 on the first day (Fig. 2). Propane is represented in RADM2 by the mechanism species HC3 which also represents other classes of VOCs, such as alcohols. The secondary chemistry of HC3 is

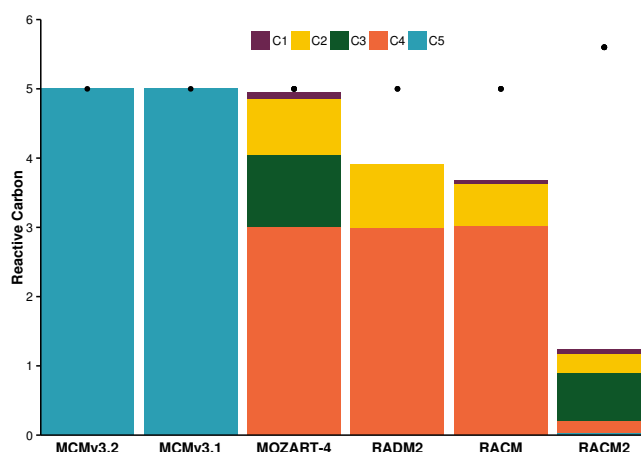


Figure 6. The distribution of reactive carbon in the products of the reaction between NO and the pentyl peroxy radical in lumped-molecule mechanisms compared to the MCM. The black dot represents the reactive carbon of the pentyl peroxy radical.

tailored to produce O_x from these different VOCs and differs from alkane degradation in the MCM v3.2 by producing less ketones in RADM2.

As will be shown in Sect. 3.3, another feature of reduced mechanisms is that the breakdown of emitted VOCs into smaller-sized degradation products is faster than the MCM. Alkanes are broken down quicker in CBM-IV, CB05, RADM2, RACM and RACM2 through a higher rate of reactive carbon loss than the MCM v3.2 (shown for pentane and octane in Fig. 8); reactive carbon is lost through reactions not conserving carbon. Despite many degradation reactions of alkanes in MOZART-4 almost conserving carbon, the organic products have less reactive carbon than the organic reactant also speeding up the breakdown of the alkane compared to the MCM v3.2.

For example, Fig. 6 shows the distribution of reactive carbon in the reactants and products from the reaction of NO with the pentyl peroxy radical in both MCMs and each lumped-molecule mechanism. In all the lumped-molecule mechanisms, the individual organic products have less reactive carbon than the organic reactant. Moreover, in RADM2, RACM and RACM2, this reaction does not conserve reactive carbon leading to faster loss rates of reactive carbon.

The faster breakdown of alkanes in lumped-molecule and lumped-structure mechanisms on the first day limits the amount of O_x produced on the second day, as less of the larger-sized degradation products are available for further degradation and O_x production.

3.3 Treatment of degradation products

The time-dependent O_x production of the different VOCs in Fig. 3 results from the varying rates at which VOCs break up into smaller fragments (Butler et al., 2011). Varying breakdown rates of the same VOCs between mechanisms could

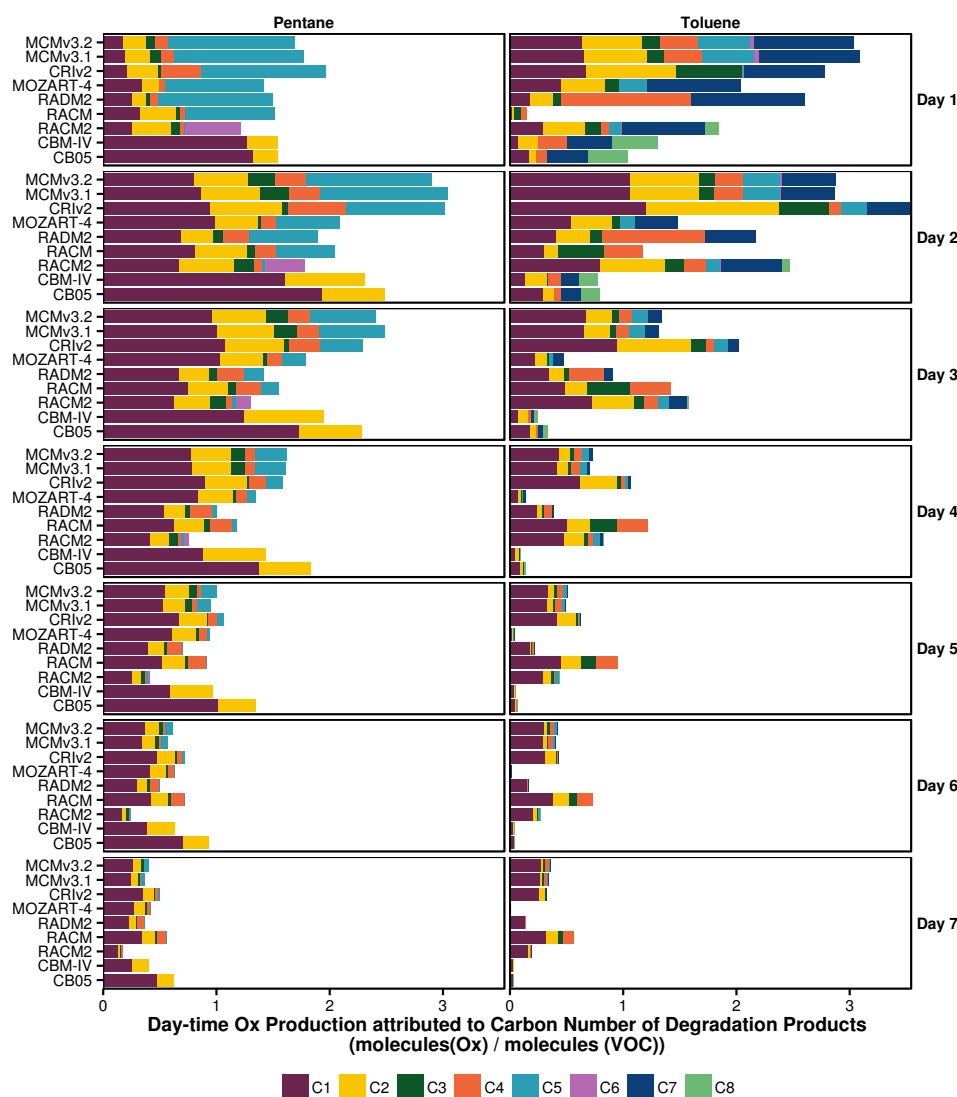


Figure 7. Day-time O_x production during pentane and toluene degradation is attributed to the number of carbon atoms of the degradation products for each mechanism.

explain the different time-dependent O_x production between mechanisms. The breakdown of pentane and toluene between mechanisms is compared in Fig. 7 by allocating the O_x production to the number of carbon atoms in the degradation products responsible for O_x production on each day of the model run in each mechanism. Some mechanism species in RADM2, RACM and RACM2 have fractional carbon numbers (Stockwell et al., 1990, 1997; Goliff et al., 2013) and O_x production from these species was reassigned as O_x production of the nearest integral carbon number.

The degradation of pentane, a five-carbon VOC, on the first day in the MCM v3.2 produces up to 50 % more O_x from degradation products also having five carbon atoms than any reduced mechanism. Moreover, the contribution of the degradation products having five carbon atoms in the MCM v3.2 is consistently higher throughout the model run than in re-

duced mechanisms (Fig. 7). Despite producing less total O_x , reduced mechanisms produce up to double the amount of O_x from degradation products with one carbon atom than in the MCM v3.2. The lower contribution of larger degradation products indicates that pentane is generally broken down faster in reduced mechanisms, consistent with the specific example shown for the breakdown of the pentyl peroxy radical in Fig. 6.

The rate of change in reactive carbon during pentane, octane and toluene degradation was determined by multiplying the rate of each reaction occurring during pentane, octane and toluene degradation by its net change in carbon, shown in Fig. 8. Pentane is broken down faster in CBM-IV, CB05, RADM2, RACM and RACM2 by losing reactive carbon more quickly than the MCM v3.2. MOZART-4 also breaks pentane down into smaller-sized products quicker

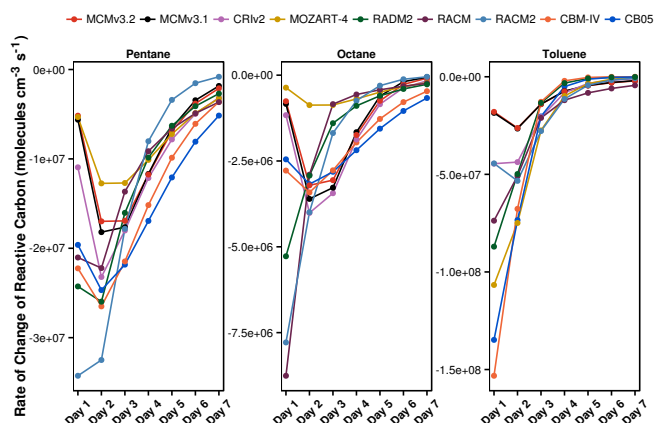


Figure 8. Daily rate of change in reactive carbon during pentane, octane and toluene degradation. Octane is represented by the five carbon species, BIGALK, in MOZART-4.

than the MCM v3.2 as reactions during pentane degradation in MOZART-4 have organic products whose carbon number is less than the organic reactant, described in Sect. 3.2.2. The faster breakdown of pentane on the first day limits the amount of reactive carbon available to produce further O_x on subsequent days leading to lower O_x production after the first day in reduced mechanisms.

Figure 3 showed that octane degradation produces peak O_x on the first day in RADM2, RACM and RACM2 in contrast to all other mechanisms where peak O_x is produced on the second day. Octane degradation in RADM2, RACM and RACM2 loses reactive carbon much faster than any other mechanism on the first day so that there are not enough degradation products available to produce peak O_x on the second day (Fig. 8). This loss of reactive carbon during alkane degradation leads to the lower accumulated ozone production from these VOCs shown in Table 3.

As seen in Fig. 3, O_x produced during toluene degradation has a high spread between the mechanisms. Figure 7 shows differing distributions of the sizes of the degradation products that produce O_x . All reduced mechanisms omit O_x production from at least one degradation fragment size which produces O_x in the MCM v3.2, indicating that toluene is also broken down more quickly in the reduced mechanisms than the more explicit mechanisms. For example, toluene degradation in RACM2 does not produce O_x from degradation products with six carbons, as is the case in the MCM v3.2. Figure 8 shows that all reduced mechanisms lose reactive carbon during toluene degradation faster than the MCM v3.2. Thus, the degradation of aromatic VOCs in reduced mechanisms are unable to produce similar amounts of O_x as the explicit mechanisms.

4 Conclusions

Tagged ozone production potentials (TOPPs) were used to compare O_x production during VOC degradation in reduced chemical mechanisms to the near-explicit MCM v3.2. First-day mixing ratios of O_3 are similar to the MCM v3.2 for most mechanisms; the O_3 mixing ratios in RACM were much lower than the MCM v3.2 due to a lack of O_x production from the degradation of aromatic VOCs. Thus, RACM may not be the appropriate chemical mechanism when simulating atmospheric conditions having a large fraction of aromatic VOCs.

The lumped-intermediate mechanism, CRI v2, produces the most similar amounts of O_x to the MCM v3.2 for each VOC. The largest differences between O_x production in CRI v2 and MCM v3.2 were obtained for aromatic VOCs; however, overall these differences were much lower than any other reduced mechanism. Thus, when developing chemical mechanisms, the technique of using lumped-intermediate species whose degradation are based upon more detailed mechanism should be considered.

Many VOCs are broken down into smaller-sized degradation products faster on the first day in reduced mechanisms than the MCM v3.2 leading to lower amounts of larger-sized degradation products that can further degrade and produce O_x . Thus, many VOCs in reduced mechanisms produce a lower maximum of O_x and lower total O_x per reactive C by the end of the run than the MCM v3.2. This lower O_x production from many VOCs in reduced mechanisms leads to lower O_3 mixing ratios compared to the MCM v3.2.

Alkanes produce maximum O_3 on the second day of simulations and this maximum is lower in reduced mechanisms than the MCM v3.2 due to the faster breakdown of alkanes into smaller-sized degradation products on the first day. The lower maximum in O_3 production during alkane degradation in reduced mechanisms leads to an underestimation of the O_3 levels downwind of VOC emissions and an underestimation of the VOC contribution to tropospheric background O_3 when using reduced mechanisms in regional or global modelling studies.

This study has determined the maximum potential of VOCs represented in reduced mechanisms to produce O_3 ; this potential may not be reached as ambient NO_x conditions may not induce NO_x -VOC-sensitive chemistry. Moreover, the maximum potential of VOCs to produce O_3 may not be reached when using these reduced mechanisms in 3-D models due to the influence of additional processes, such as mixing and meteorology. Future work shall examine the extent to which the maximum potential of VOCs to produce O_3 in reduced chemical mechanisms is reached using ambient NO_x conditions and including processes found in 3-D models.

The Supplement related to this article is available online at doi:10.5194/acp-15-8795-2015-supplement.

Acknowledgements. The authors would like to thank Mike Jenkin and William Stockwell for their helpful reviews, as well as Mark Lawrence and Peter J. H. Builtjes for valuable discussions during the preparation of this manuscript.

Edited by: R. Harley

References

- Ahmadov, R., McKeen, S., Trainer, M., Banta, R., Brewer, A., Brown, S., Edwards, P. M., de Gouw, J. A., Frost, G. J., Gilman, J., Helmig, D., Johnson, B., Karion, A., Koss, A., Langford, A., Lerner, B., Olson, J., Oltmans, S., Peischl, J., Pétron, G., Pichugina, Y., Roberts, J. M., Ryerson, T., Schnell, R., Senff, C., Sweeney, C., Thompson, C., Veres, P. R., Warneke, C., Wild, R., Williams, E. J., Yuan, B., and Zamora, R.: Understanding high wintertime ozone pollution events in an oil- and natural gas-producing region of the western US, *Atmos. Chem. Phys.*, 15, 411–429, doi:10.5194/acp-15-411-2015, 2015.
- Atkinson, R.: Atmospheric chemistry of VOCs and NO_x , *Atmos. Environ.*, 34, 2063–2101, 2000.
- Baker, A. K., Beyersdorf, A. J., Doezema, L. A., Katzenstein, A., Meinardi, S., Simpson, I. J., Blake, D. R., and Rowland, F. S.: Measurements of nonmethane hydrocarbons in 28 United States cities, *Atmos. Environ.*, 42, 170–182, 2008.
- Baklanov, A., Schlünzen, K., Suppan, P., Baldasano, J., Brunner, D., Aksoyoglu, S., Carmichael, G., Douros, J., Flemming, J., Forkel, R., Galmarini, S., Gauss, M., Grell, G., Hirtl, M., Joffre, S., Jorba, O., Kaas, E., Kaasik, M., Kallos, G., Kong, X., Korsholm, U., Kurganskiy, A., Kushta, J., Lohmann, U., Mahura, A., Manders-Groot, A., Maurizi, A., Moussiopoulos, N., Rao, S. T., Savage, N., Seigneur, C., Sokhi, R. S., Solazzo, E., Solomos, S., Sørensen, B., Tsegas, G., Vignati, E., Vogel, B., and Zhang, Y.: Online coupled regional meteorology chemistry models in Europe: current status and prospects, *Atmos. Chem. Phys.*, 14, 317–398, doi:10.5194/acp-14-317-2014, 2014.
- Bloss, C., Wagner, V., Jenkin, M. E., Volkamer, R., Bloss, W. J., Lee, J. D., Heard, D. E., Wirtz, K., Martin-Reviejo, M., Rea, G., Wenger, J. C., and Pilling, M. J.: Development of a detailed chemical mechanism (MCMv3.1) for the atmospheric oxidation of aromatic hydrocarbons, *Atmos. Chem. Phys.*, 5, 641–664, doi:10.5194/acp-5-641-2005, 2005.
- Butler, T. M., Lawrence, M. G., Taraborrelli, D., and Lelieveld, J.: Multi-day ozone production potential of volatile organic compounds calculated with a tagging approach, *Atmos. Environ.*, 45, 4082–4090, 2011.
- Carter, W. P. L.: Development of ozone reactivity scales for volatile organic compounds, *J. Air Waste Manage.*, 44, 881–899, 1994.
- Damian, V., Sandu, A., Damian, M., Potra, F., and Carmichael, G.: The kinetic preprocessor KPP – a software environment for solving chemical kinetics, *Comput. Chem. Eng.*, 26, 1567–1579, 2002.
- Derwent, R. G., Jenkin, M. E., and Saunders, S. M.: Photochemical ozone creation potentials for a large number of reactive hydrocarbons under European conditions, *Atmos. Environ.*, 30, 181–199, 1996.
- Derwent, R. G., Jenkin, M. E., Saunders, S. M., and Pilling, M. J.: Photochemical ozone creation potentials for organic compounds in Northwest Europe calculated with a master chemical mechanism, *Atmos. Environ.*, 32, 2429–2441, 1998.
- Derwent, R. G., Jenkin, M. E., Pilling, M. J., Carter, W. P. L., and Kaduwela, A.: Reactivity scales as comparative tools for chemical mechanisms, *J. Air Waste Manage.*, 60, 914–924, 2010.
- Derwent, R. G., Uttemer, S. R., Jenkin, M. E., and Shallcross, D. E.: Tropospheric ozone production regions and the intercontinental origins of surface ozone over Europe, *Atmos. Environ.*, 112, 216–224, 2015.
- Dodge, M.: Chemical oxidant mechanisms for air quality modeling: critical review, *Atmos. Environ.*, 34, 2103–2130, 2000.
- Dunker, A. M., Kumar, S., and Berzins, P. H.: A comparison of chemical mechanisms used in atmospheric models, *Atmos. Environ.*, 18, 311–321, 1984.
- Dunker, A. M., Koo, B., and Yarwood, G.: Source Apportionment of the Anthropogenic Increment to Ozone, Formaldehyde, and Nitrogen Dioxide by the Path- Integral Method in a 3D Model, *Environ. Sci. Technol.*, 49, 6751–6759, 2015.
- EEA: Air quality in Europe – 2014 report, Tech. Rep. 5/2014, European Environmental Agency, Publications Office of the European Union, doi:10.2800/22847, 2014.
- Emmerson, K. M. and Evans, M. J.: Comparison of tropospheric gas-phase chemistry schemes for use within global models, *Atmos. Chem. Phys.*, 9, 1831–1845, doi:10.5194/acp-9-1831-2009, 2009.
- Emmons, L. K., Walters, S., Hess, P. G., Lamarque, J.-F., Pfister, G. G., Fillmore, D., Granier, C., Guenther, A., Kinnison, D., Laepple, T., Orlando, J., Tie, X., Tyndall, G., Wiedinmyer, C., Baughcum, S. L., and Kloster, S.: Description and evaluation of the Model for Ozone and Related chemical Tracers, version 4 (MOZART-4), *Geosci. Model Dev.*, 3, 43–67, doi:10.5194/gmd-3-43-2010, 2010.
- Foster, P. N., Prentice, I. C., Morfopoulos, C., Siddall, M., and van Weele, M.: Isoprene emissions track the seasonal cycle of canopy temperature, not primary production: evidence from remote sensing, *Biogeosciences*, 11, 3437–3451, doi:10.5194/bg-11-3437-2014, 2014.
- Gery, M. W., Whitten, G. Z., Killus, J. P., and Dodge, M. C.: A photochemical kinetics mechanism for urban and regional scale computer modeling, *J. Geophys. Res.*, 94, 12925–12956, 1989.
- Goliff, W. S., Stockwell, W. R., and Lawson, C. V.: The regional atmospheric chemistry mechanism, version 2, *Atmos. Environ.*, 68, 174–185, 2013.
- Goliff, W. S., Luria, M., Blake, D. R., Zielinska, B., Hallar, G., Valente, R. J., Lawson, C. V., and Stockwell, W. R.: Nighttime air quality under desert conditions, *Atmos. Environ.*, 114, 102–111, 2015.
- Harwood, M., Roberts, J., Frost, G., Ravishankara, A., and Burkholder, J.: Photochemical studies of $\text{CH}_3\text{C}(\text{O})\text{OONO}_2$ (PAN) and $\text{CH}_3\text{CH}_2\text{C}(\text{O})\text{OONO}_2$ (PPN): NO_3 quantum yields, *J. Phys. Chem. A*, 107, 1148–1154, 2003.
- Hogo, H. and Gery, M.: User's guide for executing OZIPM-4 (Ozone Isopleth Plotting with Optional Mechanisms, Version 4) with CBM-IV (Carbon-Bond Mechanisms-IV) or optional mechanisms. Volume 1. Description of the ozone isopleth plotting package. Version 4, Tech. rep., US Environmental Protection Agency, Durham, North Carolina, USA, 1989.
- Hou, X., Zhu, B., Fei, D., and Wang, D.: The impacts of summer monsoons on the ozone budget of the atmospheric boundary

- layer of the Asia-Pacific region, *Sci. Total Environ.*, 502, 641–649, 2015.
- HTAP: Hemispheric Transport of Air Pollution 2010, Part A: Ozone and Particulate Matter, Air Pollution Studies No.17, Geneva, Switzerland, 2010.
- Jenkin, M. E. and Clemitshaw, K. C.: Ozone and other secondary photochemical pollutants: chemical processes governing their formation in the planetary boundary layer, *Atmos. Environ.*, 34, 2499–2527, 2000.
- Jenkin, M. E., Saunders, S. M., and Pilling, M. J.: The tropospheric degradation of volatile organic compounds: a protocol for mechanism development, *Atmos. Environ.*, 31, 81–104, 1997.
- Jenkin, M. E., Saunders, S. M., Wagner, V., and Pilling, M. J.: Protocol for the development of the Master Chemical Mechanism, MCM v3 (Part B): tropospheric degradation of aromatic volatile organic compounds, *Atmos. Chem. Phys.*, 3, 181–193, doi:10.5194/acp-3-181-2003, 2003.
- Jenkin, M. E., Watson, L. A., Utembe, S. R., and Shallcross, D. E.: A Common Representative Intermediates (CRI) mechanism for VOC degradation. Part 1: Gas phase mechanism development, *Atmos. Environ.*, 42, 7185–7195, 2008.
- Kleinman, L. I.: Seasonal dependence of boundary layer peroxide concentration: the low and high NO_x regimes, *J. Geophys. Res.*, 96, 20721–20733, 1991.
- Kleinman, L. I.: Low and high NO_x tropospheric photochemistry, *J. Geophys. Res.*, 99, 16831–16838, 1994.
- Koss, A. R., de Gouw, J., Warneke, C., Gilman, J. B., Lerner, B. M., Graus, M., Yuan, B., Edwards, P., Brown, S. S., Wild, R., Roberts, J. M., Bates, T. S., and Quinn, P. K.: Photochemical aging of volatile organic compounds associated with oil and natural gas extraction in the Uintah Basin, UT, during a wintertime ozone formation event, *Atmos. Chem. Phys.*, 15, 5727–5741, doi:10.5194/acp-15-5727-2015, 2015.
- Kuhn, M., Bultjes, P. J. H., Poppe, D., Simpson, D., Stockwell, W. R., Andersson-Sköld, Y., Baart, A., Das, M., Fiedler, F., Hov, Ø., Kirchner, F., Makar, P. A., Milford, J. B., Roemer, M. G. M., Ruhnke, R., Strand, A., Vogel, B., and Vogel, H.: Intercomparison of the gas-phase chemistry in several chemistry and transport models, *Atmos. Environ.*, 32, 693–709, 1998.
- Li, J., Georgescu, M., Hyde, P., Mahalov, A., and Moustouli, M.: Achieving accurate simulations of urban impacts on ozone at high resolution, *Environ. Res. Lett.*, 9, 114019, doi:10.1088/1748-9326/9/11/114019, 2014.
- Lidster, R. T., Hamilton, J. F., Lee, J. D., Lewis, A. C., Hopkins, J. R., Punjabi, S., Rickard, A. R., and Young, J. C.: The impact of monoaromatic hydrocarbons on OH reactivity in the coastal UK boundary layer and free troposphere, *Atmos. Chem. Phys.*, 14, 6677–6693, doi:10.5194/acp-14-6677-2014, 2014.
- Rickard, A., Young, J., Pilling, M., Jenkin, M., Pascoe, S., and Saunders, S.: The Master Chemical Mechanism Version MCM v3.2, available at: <http://mcm.leeds.ac.uk/MCMv3.2/>, last access: 15 July 2015.
- Sander, R., Kerkweg, A., Jöckel, P., and Lelieveld, J.: Technical note: The new comprehensive atmospheric chemistry module MECCA, *Atmos. Chem. Phys.*, 5, 445–450, doi:10.5194/acp-5-445-2005, 2005.
- Saunders, S. M., Jenkin, M. E., Derwent, R. G., and Pilling, M. J.: Protocol for the development of the Master Chemical Mechanism, MCM v3 (Part A): tropospheric degradation of non-aromatic volatile organic compounds, *Atmos. Chem. Phys.*, 3, 161–180, doi:10.5194/acp-3-161-2003, 2003.
- Sillman, S.: The relation between ozone, NO_x and hydrocarbons in urban and polluted rural environments, *Atmos. Environ.*, 33, 1821–1845, 1999.
- Stevenson, D. S., Young, P. J., Naik, V., Lamarque, J.-F., Shindell, D. T., Voulgarakis, A., Skeie, R. B., Dalsoren, S. B., Myhre, G., Berntsen, T. K., Folberth, G. A., Rumbold, S. T., Collins, W. J., MacKenzie, I. A., Doherty, R. M., Zeng, G., van Noije, T. P. C., Strunk, A., Bergmann, D., Cameron-Smith, P., Plummer, D. A., Strode, S. A., Horowitz, L., Lee, Y. H., Szopa, S., Sudo, K., Nagashima, T., Josse, B., Cionni, I., Righi, M., Eyring, V., Conley, A., Bowman, K. W., Wild, O., and Archibald, A.: Tropospheric ozone changes, radiative forcing and attribution to emissions in the Atmospheric Chemistry and Climate Model Intercomparison Project (ACCMIP), *Atmos. Chem. Phys.*, 13, 3063–3085, doi:10.5194/acp-13-3063-2013, 2013.
- Stockwell, W. R., Middleton, P., Chang, J. S., and Tang, X.: The second generation regional acid deposition model chemical mechanism for regional air quality modeling, *J. Geophys. Res.*, 95, 16343–16367, 1990.
- Stockwell, W. R., Kirchner, F., Kuhn, M., and Seinfeld, S.: A new mechanism for regional atmospheric chemistry modeling, *J. Geophys. Res.-Atmos.*, 102, 25847–25879, 1997.
- Watson, L. A., Shallcross, D. E., Utembe, S. R., and Jenkin, M. E.: A Common Representative Intermediates (CRI) mechanism for VOC degradation. Part 2: Gas phase mechanism reduction, *Atmos. Environ.*, 42, 7196–7204, 2008.
- Yarwood, G., Rao, S., Yocke, M., and Whitten, G. Z.: Updates to the Carbon Bond Chemical Mechanism: CB05, Tech. rep., US Environmental Protection Agency, Novato, California, USA, 2005.

Chapter 7

Paper 2:

Chapter 8

Paper 3:

Chapter 9

Publication List

Appendix

